

## RESEARCH ARTICLE

# *Lhx2* is a direct NF- $\kappa$ B target gene that promotes primary hair follicle placode down-growth

Philip Tomann<sup>1</sup>, Ralf Paus<sup>2,3</sup>, Sarah E. Millar<sup>4</sup>, Claus Scheidereit<sup>1</sup> and Ruth Schmidt-Ullrich<sup>1,\*</sup>

## ABSTRACT

In the epidermis of mice lacking transcription factor nuclear factor-kappa B (NF- $\kappa$ B) activity, primary hair follicle (HF) pre-placode formation is initiated without progression to proper placodes. NF- $\kappa$ B modulates WNT and SHH signaling at early stages of HF development, but this does not fully account for the phenotypes observed upon NF- $\kappa$ B inhibition. To identify additional NF- $\kappa$ B target genes, we developed a novel method to isolate and transcriptionally profile primary HF placodes with active NF- $\kappa$ B signaling. In parallel, we compared gene expression at the same developmental stage in NF- $\kappa$ B-deficient embryos and controls. This uncovered novel NF- $\kappa$ B target genes with potential roles in priming HF placodes for down-growth. Importantly, we identify *Lhx2* (encoding a LIM/homeobox transcription factor) as a direct NF- $\kappa$ B target gene, loss of which replicates a subset of phenotypes seen in NF- $\kappa$ B-deficient embryos. *Lhx2* and *Tgfb2* knockout embryos exhibit very similar abnormalities in HF development, including failure of the E-cadherin suppression required for follicle down-growth. We show that TGF $\beta$ 2 signaling is impaired in NF- $\kappa$ B-deficient and *Lhx2* knockout embryos and that exogenous TGF $\beta$ 2 rescues the HF phenotypes in *Lhx2* knockout skin explants, indicating that it operates downstream of LHX2. These findings identify a novel NF- $\kappa$ B/LHX2/TGF $\beta$ 2 signaling axis that is crucial for primary HF morphogenesis, which may also function more broadly in development and disease.

**KEY WORDS:** NF- $\kappa$ B, LHX2, Hair follicle, TGF $\beta$ 2, Cell migration, E-cadherin, EDA-A1, EDAR, Mouse, Embryo, Placode, Stem cell

## INTRODUCTION

Hair follicle (HF) development is initiated by a reciprocal signaling interplay between the surface epithelium and the underlying mesenchyme that results in local epithelial thickenings, the HF placodes (Biggs and Mikkola, 2014; Fuchs, 2007; Hardy, 1992; Schmidt-Ullrich and Paus, 2005; Schneider et al., 2009; Sennett and Rendl, 2012). The regular array of placodes is thought to be mediated by a reaction-diffusion system of competing placode activator and inhibitor morphogens (Bazzi et al., 2007; Jiang et al., 2004; Mou et al., 2006; Sick et al., 2006). Mouse HF development occurs in three major waves, with primary (guard, tylotrich) HFs forming at embryonic day (E) 14.5, and awl/auchene and zigzag HFs starting to generate at E16.5 and E18.5, respectively. These

distinct waves are differentially regulated at the molecular level. Epidermal and dermal canonical WNT/ $\beta$ -catenin signaling is required to initiate the development of all hair types, whereas bone morphogenetic protein (BMP) signals generally function to impede placode development (Andl et al., 2002; Botchkarev et al., 1999; Chen et al., 2012; Mou et al., 2006; Oro and Scott, 1998; Zhang et al., 2008, 2009a). In addition to WNT/ $\beta$ -catenin signaling, primary HF formation specifically depends on the activity of the TNF family member EDA-A1 (ectodysplasin-A1; also known as EDA) in the epidermis (Headon and Overbeek, 1999; Kere et al., 1996; Laurikkala et al., 2002; Schmidt-Ullrich et al., 2001, 2006). *Eda-A1* ligand and its receptor *Edar* (ectodysplasin receptor) are both direct target genes of WNT/ $\beta$ -catenin, and EDA-A1-EDAR interaction results in downstream activation of the transcription factor nuclear factor-kappa B (NF- $\kappa$ B) in developing primary placodes (Kumar et al., 2001; Laurikkala et al., 2002; Schmidt-Ullrich et al., 2006; Yan et al., 2000; Zhang et al., 2009a).

In the absence of EDA-A1/EDAR/NF- $\kappa$ B signaling, WNT/ $\beta$ -catenin initiates HF placode formation in a messy pre-pattern up to the pre-placode stage (hair morphogenesis stage 0/1; Paus et al., 1999) in which a subset of placode markers is already expressed, but subsequent down-growth and morphogenesis are arrested (Schmidt-Ullrich et al., 2006; Zhang et al., 2009a). The ill-defined borders of these pre-placodes revealed a role for EDA-A1/EDAR/NF- $\kappa$ B signaling in pattern refinement of early WNT/ $\beta$ -catenin activity in primary HF placodes by upregulating expression of WNT inhibitors such as DKK4 (Bazzi et al., 2007; Fliniaux et al., 2008; Zhang et al., 2009a). Furthermore, a suggested function for EDA-A1/EDAR/NF- $\kappa$ B in suppressing placode-inhibitory BMP signals within primary placodes might be important to maintain HF fate and prevent premature differentiation (Mou et al., 2006; Pummila et al., 2007). With the exception of recombinant Fc-EDA-A1, TNF $\alpha$  and to some extent high doses of the BMP inhibitor noggin, other potential effectors downstream of EDA-A1 signaling, such as SHH or the chemokines CXCL10 and 11, failed to rescue primary HF placode formation in EDA-A1-deficient embryonic skin explants (Laurikkala et al., 2002; Lefebvre et al., 2012; Pummila et al., 2007; Schmidt-Ullrich et al., 2006). This indicates that the known EDA-A1/EDAR/NF- $\kappa$ B target genes are not sufficient to define the apparently complex role of EDA-A1/EDAR/NF- $\kappa$ B signaling in primary hair placode development. Therefore additional NF- $\kappa$ B-dependent factors must be required to establish proper conditions for placode down-growth beyond initiation, patterning and BMP inhibition.

Previous microarray analyses have identified some NF- $\kappa$ B target genes. However, all these studies utilized either whole skin (epidermis and dermis) or skin explants that had been treated with recombinant EDA-A1 or left untreated (Bazzi et al., 2007; Cui et al., 2002, 2006; Laurikkala et al., 2002; Lefebvre et al., 2012; Mou et al., 2006; Pummila et al., 2007). Therefore, placode-specific genes that are expressed at low levels might have been missed. To

<sup>1</sup>Department of Signal Transduction in Tumor Cells, Max-Delbrück-Center (MDC) for Molecular Medicine, Berlin 13092, Germany. <sup>2</sup>Department of Dermatology, University of Münster, Münster 48149, Germany. <sup>3</sup>Dermatological Science Research Group, Centre for Dermatology Research, Institute of Inflammation and Repair, University of Manchester, Manchester M13 9PL, UK. <sup>4</sup>Departments of Dermatology and Cell and Developmental Biology, Perelman School of Medicine, University of Pennsylvania, Philadelphia, PA 19104, USA.

\*Author for correspondence (rschmidt@mdc-berlin.de)

Received 11 September 2015; Accepted 19 February 2016

identify additional genes functioning downstream of NF- $\kappa$ B, we established a gene signature that is both placode keratinocyte specific, and NF- $\kappa$ B dependent. To this end, we generated a novel NF- $\kappa$ B-EGFP reporter mouse line. This allowed us to isolate and purify hair placode keratinocytes and to set up a detailed gene expression profile specifically of NF- $\kappa$ B-active primary hair placodes. In parallel, to identify NF- $\kappa$ B-dependent genes, we profiled gene expression in NF- $\kappa$ B-inhibited compared with control embryonic mouse epidermis.

HF placode formation and down-growth is a complex process that depends on changes in local keratinocyte adhesion, migration, polarity and proliferation, as well as modifications in the surrounding extracellular matrix (ECM). In addition to expected NF- $\kappa$ B targets, such as genes that control NF- $\kappa$ B and WNT signaling, we identified a significant number of new targets, including ECM components, genes involved in cell adhesion and migration, and stem cell-associated genes. Of particular interest, we identified the gene encoding the LIM-homeodomain transcription factor LHX2 as a novel NF- $\kappa$ B target gene in HF placodes. LHX2 was originally shown to control patterning, cell fate decisions and axon guidance during embryonic brain development (Bulchand et al., 2001; Hirota and Mombaerts, 2004; Mangale et al., 2008; Porter et al., 1997; Shetty et al., 2013). However, LHX2 also plays an important role in HF stem cell growth and maintenance within the stem cell niche by regulating cell adhesion and cytoskeletal dynamics (Folgueras et al., 2013; Rhee et al., 2006). A requirement of LHX2 for anagen induction has been indicated as well (Törnqvist et al., 2010). LHX2 is expressed in stage 0 and stage 1 embryonic HF placodes that also display NF- $\kappa$ B activity, and *Lhx2*-deficient embryos have reduced numbers of HFs (Rhee et al., 2006; Törnqvist et al., 2010). These data suggest a role for LHX2 in HF morphogenesis. However, as *Lhx2*-deficient embryos die around E15–E16, when primary HF development is still ongoing, further detailed morphological and molecular analyses of HF development have not previously been pursued (Porter et al., 1997; Rhee et al., 2006). A more recent study using a mouse line harboring a hypomorphic *Lhx2* allele examined HF development at later time points, but only confirmed previous assumptions regarding a possible role of LHX2 in HF development (Törnqvist et al., 2010). Our results now demonstrate an essential role for LHX2 in preparing primary hair pre-placodes for down-growth downstream of EDA-A1/EDAR/NF- $\kappa$ B signaling.

## RESULTS

### NF- $\kappa$ B-dependent gene signature in primary HF placodes reveals a multifunctional role for NF- $\kappa$ B in HF development

To obtain a gene signature for NF- $\kappa$ B-active primary HF placodes, we generated an NF- $\kappa$ B-responsive reporter mouse line that uses EGFP as read-out for *in vivo* NF- $\kappa$ B activity ( $\kappa$ -EGFP; Fig. 1A; Table S1). The expression pattern of EGFP was identical to that observed in a previously produced NF- $\kappa$ B reporter line (Schmidt-Ullrich et al., 2001, 1996), including strong NF- $\kappa$ B activity in developing HF placode keratinocytes (Fig. 1A; Fig. S1A). Epidermis from E14.5  $\kappa$ -EGFP embryos was harvested, EGFP-expressing HF placode keratinocytes were purified by fluorescence-activated cell sorting (FACS), and total placode keratinocyte RNA was processed for microarray analysis (Fig. 1B,C; Fig. S1B; Table S1). To exclude contamination of our epidermal samples with mesenchymal cell types, we analyzed mRNA expression of four dermal markers, *Bmp4*, *Colla1* (collagen 1 alpha1), *Irx1* (Iroquois homeobox 1) and *Ngfr* (nerve growth factor receptor; also known as p75NTR), which either revealed absence (*Colla1*, *Ngfr*) or very low expression levels (*Bmp4*, *Irx1*) of these markers (Fig. S2A) (see

<http://hair-gel.net/>; Botchkareva et al., 1999; St-Jacques et al., 1998). The resulting NF- $\kappa$ B-active placode-specific gene signature was aligned with an epidermis-specific NF- $\kappa$ B-dependent gene signature that was obtained from microarray transcriptional profiling of epidermis from embryos with suppressed NF- $\kappa$ B activity ( $\Delta N$ ) compared with littermate controls at E14.5 (Table S2). These experiments allowed us to identify 74 genes that are specifically expressed in NF- $\kappa$ B-active placode cells, and are directly or indirectly dependent on NF- $\kappa$ B signaling (Fig. 1B).

We validated the data from our profiling experiments by comparison with previously described NF- $\kappa$ B targets and functions in the context of HF formation, confirming the sensitivity and specificity of our experimental strategy (Fig. 1C). These genes included those in the SHH signaling pathway (*Shh*, *Gli1*, *Ptch2*, *Etv4* and *Etv5*); known NF- $\kappa$ B target genes such as the NF- $\kappa$ B family member *RelB* (Table S1), *Tnfaip3* (encoding the ubiquitin editing enzyme A20), *Tnf* (TNF $\alpha$ ), *Ltb* (lymphotoxin  $\beta$ ), *Foxi3* (forkhead box I3), chemokine *Cxcl11*; and regulators of the WNT pathway, such as *Dkk4* and also a newly identified NF- $\kappa$ B target, *Wif1* (WNT inhibitory factor 1) (Fig. 1C; Fig. S3A–C) (Bazzi et al., 2007; Cui et al., 2006; Fliniaux et al., 2008; Lefebvre et al., 2012; Lettice et al., 2012; Mao et al., 2009; Schmidt-Ullrich et al., 2006; Shirokova et al., 2013; Zhang et al., 2009a,b). A striking number of genes that we identified as potential NF- $\kappa$ B target genes encode ECM components [*Frem1* (FRAS1 related extracellular matrix 1), *Mmp9* (metalloproteinase 9), *Tnc* (tenascin C)], receptors and genes implicated in cell migration [*Prokr2* (prokineticin receptor 2), *Nrp2* (neuropilin 2), *Cd74* (HLA class II histocompatibility antigen gamma chain or HLA-DR antigen-associated invariant chain; which can act as a receptor for macrophage migration inhibitory factor)] or are involved in cell-adhesion, such as *Ncam1* and *Madcam1* (Fig. 1C). Although *Frem1*, *Madcam1* and *Mmp9* have previously been described as NF- $\kappa$ B target genes (Takeuchi and Baichwal, 1995; Yoon et al., 2012; Yoshizaki et al., 1998), *Prokr2*, *Nrp2*, *Cd74* and *Ncam1* are new potential targets. Importantly, novel NF- $\kappa$ B-regulated genes with special relevance for hair biology, such as transcription factors *Lhx2* (LIM homeobox protein 2) (Folgueras et al., 2013; Mardaryev et al., 2011; Rhee et al., 2006; Törnqvist et al., 2010), *Sox9* (SRY-box 9) (Nowak et al., 2008; Vidal et al., 2005), *Trps1* (trichorhinophalangeal syndrome 1) (Fantauzzo et al., 2008a,b; Kunath et al., 2002; Malik et al., 2002; Momeni et al., 2000) and *Sox21* (SRY-box 21) (Kiso et al., 2009), were also identified (Fig. 1C). A role for LHX2 in primary HF placode down-growth will be described in more detail below.

A number of previously suggested or confirmed NF- $\kappa$ B target genes were upregulated in HF placodes at E14.5, but were not significantly controlled by NF- $\kappa$ B at this time point (Fig. 1C). These comprised the BMP signaling regulator *Ctgf* (connective tissue growth factor) (Pummila et al., 2007), *Wnt10b* (Zhang et al., 2009a) and bona fide NF- $\kappa$ B target *Nfkbia* (NF- $\kappa$ B inhibitor of  $\kappa$ B $\alpha$ , I $\kappa$ B $\alpha$ ) (Le Bail et al., 1993). *Ctgf* expression might also be regulated by WNT/ $\beta$ -catenin, which is very active in HF placodes at E14.5. For *Wnt10b*, we showed previously that it is only regulated by NF- $\kappa$ B at E15.5 when primary HF stage 1 placodes enter the germ stage (stage 2) (Zhang et al., 2009a). *Nfkbia* was expected to be downregulated in  $\Delta N$  embryos, but the lack of differential regulation might be due to detection of the truncated human I $\kappa$ B $\alpha$  ( $\Delta N$ ) by the mouse array used for our analysis (Schmidt-Ullrich et al., 2001, 2006).

To verify placode-specific expression and dependence on NF- $\kappa$ B activity, candidate targets were examined by quantitative real time-PCR (qRT-PCR) for enrichment in developing primary HF placodes and for differential expression in  $\Delta N$  versus control epidermis at

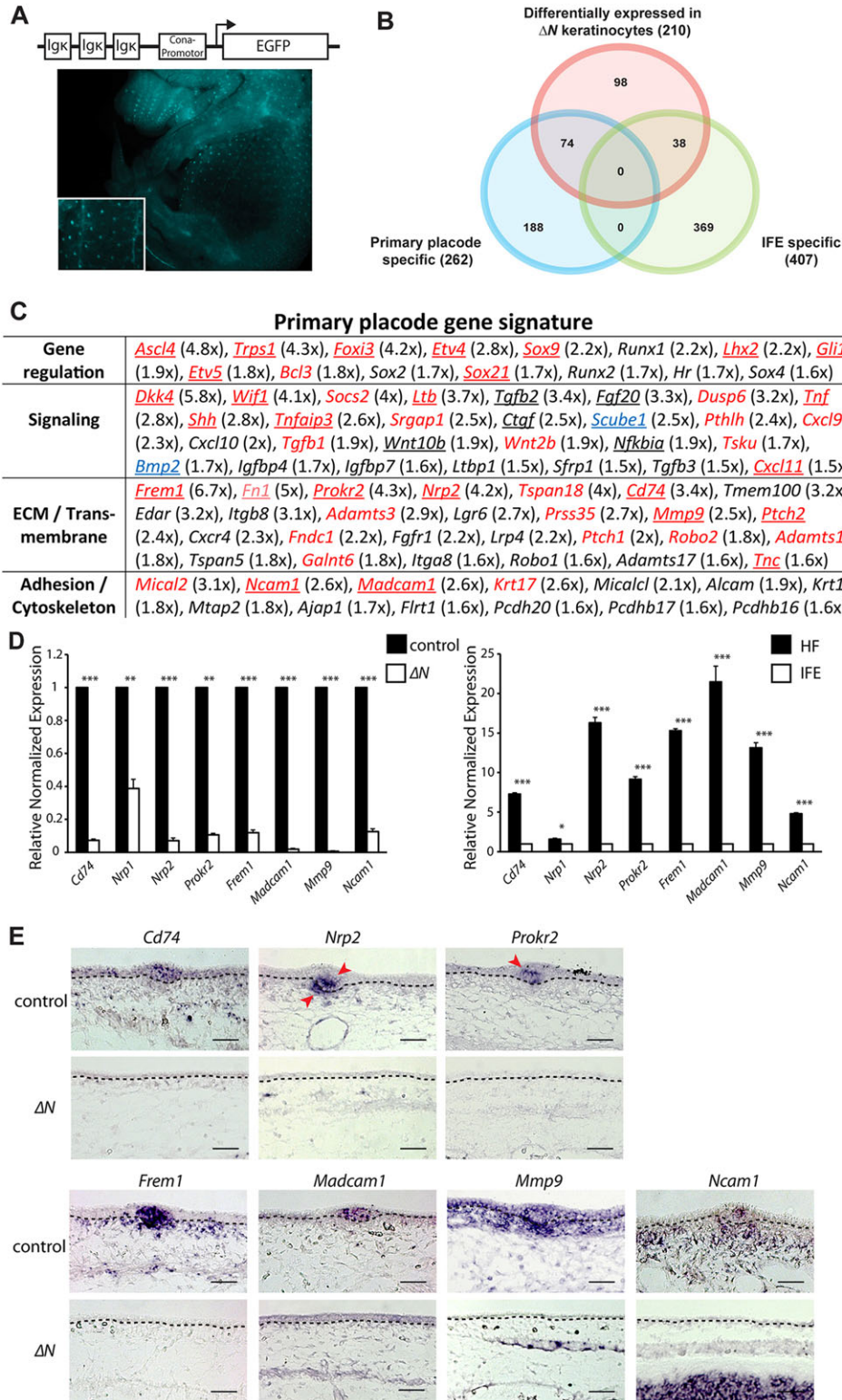


**Fig. 1. NF- $\kappa$ B-dependent gene signature in primary HF placodes reveals a multifunctional role.** (A) Generation of an NF- $\kappa$ B-responsive EGFP reporter mouse line ( $\kappa$ -EGFP). EGFP expression was observed in the developing HF and in blood vessels of the skin at E14.5. Inset shows high magnification of skin with EGFP-expressing placodes. (B) Venn diagram illustrating overlap of genes up- or downregulated in primary HF placodes with differentially expressed genes in  $\Delta N$  versus control epidermal keratinocytes. For full list of microarray data, see Table S1. (C) Primary HF placode-specific gene signature obtained from microarray analysis of sorted EGFP-positive keratinocytes at E14.5. Genes mentioned in the text are underlined. Functional categories with representative examples of mRNAs upregulated  $\geq 1.5\times$  are listed. Fold differences between placodes and interfollicular epidermis (EGFP negative) are indicated in parentheses. Genes highlighted in red were downregulated and in blue upregulated in  $\Delta N$ -positive epidermal keratinocytes. Genes in black were specifically enriched in HF placodes, but not regulated by NF- $\kappa$ B in a significant manner. Note that *Fn1* (in light red) expression is enriched  $5\times$  in HF placodes, but is only weakly downregulated in  $\Delta N$  versus controls ( $\sim 1.3\times$ ). (D) Quantitative real-time PCR (qRT-PCR) analysis using either RNA samples from epidermal keratinocytes of  $n=3$  control or  $\Delta N$  embryos at E14.5 (left graph), or from FACS-sorted EGFP-positive (HF) or EGFP-negative (IFE) keratinocytes of  $\kappa$ -EGFP embryos at E14.5 (right graph). Statistical analyses were performed using a two-tailed unpaired *t*-test. Data are presented as mean  $\pm$  s.e.m. \* $P<0.05$ ; \*\* $P<0.01$ ; \*\*\* $P<0.001$ . (E) *In situ* hybridization for the indicated mRNA probes using sagittal skin sections of  $n=3$  control and  $\Delta N$  embryos at E14.5. Arrowheads indicate expression in HF placodes and dermal papilla (Nrp2); dashed line delineates the dermal-epidermal boundary. Scale bars: 50  $\mu$ m.

E14.5 (Fig. 1D; Fig. S3). qRT-PCR revealed a significant dependence on NF- $\kappa$ B activity for all candidate target genes, including those that regulate cell migration and adhesion (Fig. 1D,E; Fig. 3; Fig. S3A,B). To identify potential direct targets, the genomic regions of differentially expressed genes were screened for putative NF- $\kappa$ B-binding sites using the JASPER database (<http://jaspar.genereg.net/>). We also used the ECR browser (<http://ecrbrowser.decode.org>) to check for NF- $\kappa$ B-binding site conservation across

species (Table S3). These analyses verified that 96% of the potential target genes contained at least one conserved NF- $\kappa$ B-binding site (Table S3). Potential binding sites were further confirmed by chromatin immunoprecipitation (ChIP) for *Lhx2*, *Sox9*, *Trps1* and *Mmp9* (see below; data not shown; see also Table S3 and supplementary Materials and Methods). Interestingly, 57% of the NF- $\kappa$ B-regulated genes found in our gene chip analysis were also identified by ChIP as direct NF- $\kappa$ B targets in Hodgkin lymphoma

cell lines (de Oliveira et al., 2016) (Table S3). This suggests that physiological NF- $\kappa$ B functions required for primary HF placode formation in mice may in part contribute to human tumor growth and/or survival.

HF placode-specific mRNA expression of identified potential NF- $\kappa$ B target genes was further validated by *in situ* hybridization (ISH) on control skin and  $\Delta N$  skin samples at E14.5 (Fig. 1E; Fig. S3C). Interestingly, mRNA expression of *Bmp2* and *Scube1* (signal peptide-CUB domain EGF-related 1), a potential SHH and BMP signaling regulator (Johnson et al., 2012; Tsao et al., 2013), was expanded in the absence of epidermal NF- $\kappa$ B activity. ISH revealed that *Bmp2* and *Scube1* were ubiquitously expressed in the epidermis of  $\Delta N$  embryos at E14.5, whereas expression was restricted to primary HF placodes in controls (Fig. S3C). This suggests that NF- $\kappa$ B activity might be indirectly required for restricting *Bmp2* and *Scube1* expression to HF placodes. Some of the NF- $\kappa$ B-regulated genes were also expressed in the dermal condensate (*Nrp2*, *Mmp9*, *Tnc*) and at the interface between placode and dermal condensate (*Mmp9*, *Tnc*) (Fig. 1E; Fig. S3C). This latter group of differentially regulated genes strongly points to a role for

NF- $\kappa$ B in ECM modulation and in cell migration in order to allow placode down-growth, and further suggests additional non-cell-autonomous mechanisms by which epithelial NF- $\kappa$ B signaling modulates gene expression in other cell types. Note that six genes were specifically upregulated in the interfollicular epidermis (IFE), but downregulated by NF- $\kappa$ B in placodes (Table S4). However, none of these genes has any known functions in IFE development or maintenance, suggesting that NF- $\kappa$ B is not required for downregulating important IFE regulatory genes in order to promote HF formation.

### NF- $\kappa$ B directly regulates *Lhx2* expression and acts in concert with LHX2 to control genes involved in cell migration during placode down-growth

Although the novel NF- $\kappa$ B targets *Lhx2* and *Sox9* may suggest an interesting role for NF- $\kappa$ B in stem cell biology, these HF stem cell markers have not previously been associated with early stages of placode formation. mRNA expression of *Lhx2* and *Sox9* was strictly dependent on NF- $\kappa$ B activity in primary HF placodes at E14.5 (Fig. 2A; Fig. S3A–C). In line with this, the promoter of each of

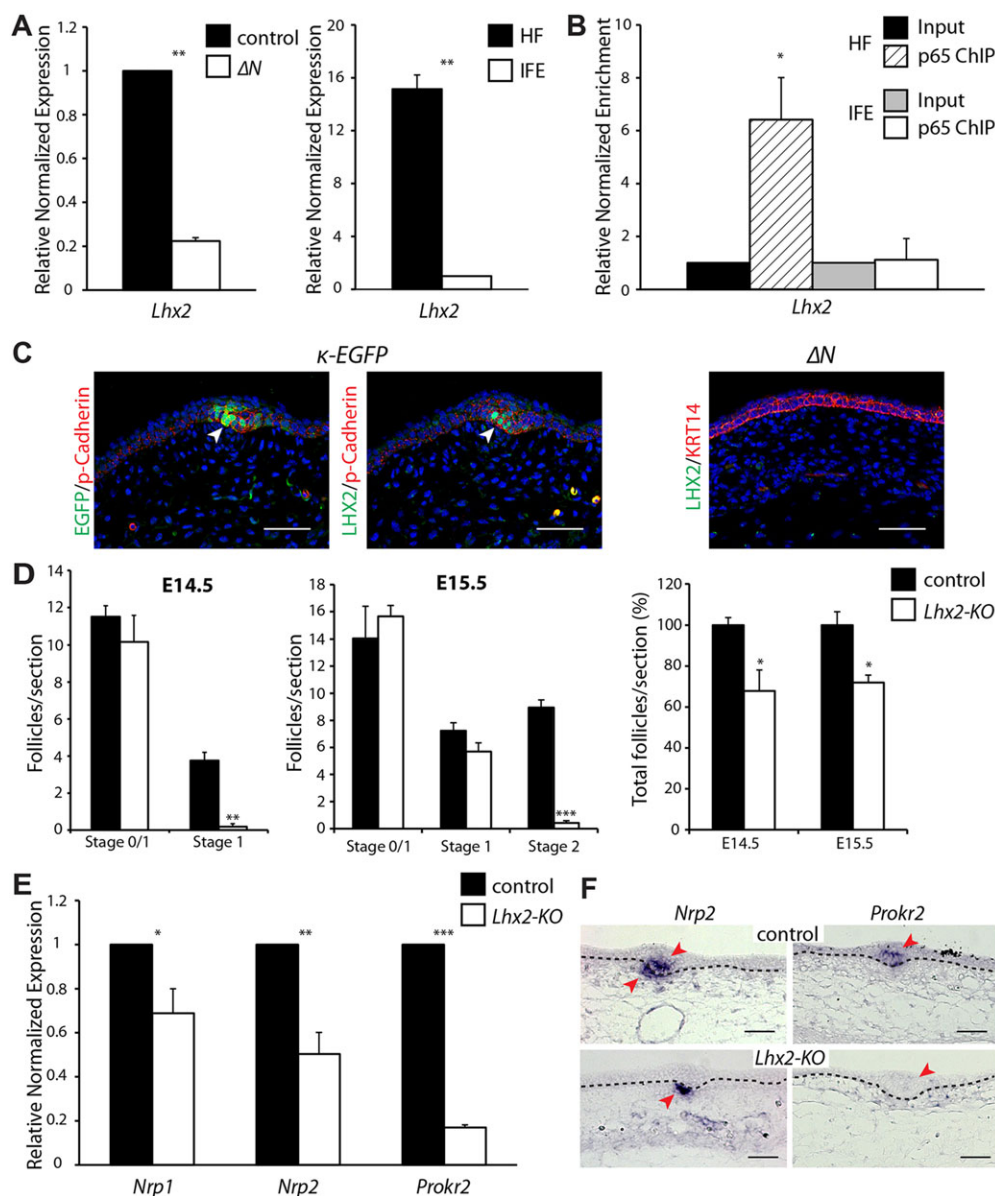


**Fig. 2. *Lhx2* is a direct target gene of NF- $\kappa$ B during primary placode formation and acts in concert with NF- $\kappa$ B to regulate genes involved in cell migration.** (A) qRT-PCR of *Lhx2* mRNA expression from epidermal keratinocytes of  $n=3$  control or  $\Delta N$  embryos (left graph), or from EGFP-positive placode and EGFP-negative IFE keratinocytes (right graph) at E14.5. (B) NF- $\kappa$ B p65-specific ChIP assays using EGFP-positive placode and EGFP-negative IFE keratinocyte extracts from  $\kappa$ -EGFP embryos at E14.5, and *Lhx2* and control *Gapdh* primers. (C) Immunostaining on serial sagittal back skin sections of  $n=3$   $\kappa$ -EGFP and  $\Delta N$  mice at E14.5 using antibodies against EGFP, P-cadherin (cadherin 3), LHX2 and KRT14. Arrowheads indicate expression in HF placodes. Blue, nuclear DAPI staining. (D) Analysis of primary HF development in *Lhx2*-KO mice revealed a dramatic reduction of stage 1 (E14.5; left graph) and stage 2 (E15.5; middle graph) primary HF. Overall primary HF density in *Lhx2*-KO embryos at E14.5 and E15.5 was reduced by ~30% (right graph). The graphs show quantification from multiple back skin sections of three biological replicates. (E) qRT-PCR for selected NF- $\kappa$ B target genes involved in cell migration using mRNA isolated from epidermal keratinocytes of either *Lhx2*-KO or control embryos at E14.5. (F) *In situ* hybridization for *Nrp2* and *Prokr2* mRNA on sagittal skin sections of control and *Lhx2*-KO embryos at E14.5. Arrowheads indicate mRNA expression in HF placodes and also in the dermal papilla for *Nrp2*; dashed line delineates dermal-epidermal boundaries. Scale bars: 50  $\mu$ m. All statistical analyses (A,B,D,E) were performed using two-tailed unpaired t-test. Data are presented as mean $\pm$ s.e.m. \* $P<0.05$ ; \*\* $P<0.01$ ; \*\*\* $P<0.001$ .

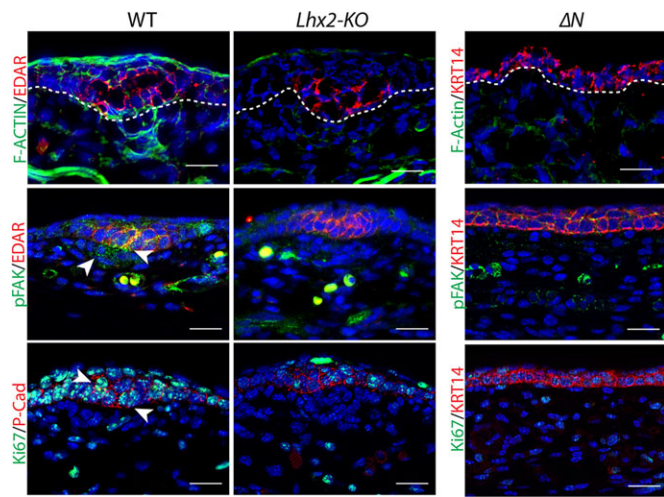


**Fig. 3.** *ΔN* and *Lhx2*-KO mice exhibit keratinocyte migratory and proliferative defects in the down-growing primary HF placode.

Immunostaining on sagittal sections of  $n=3$  control, *Lhx2*-KO and *ΔN* embryos at E14.5. Cytoskeletal organization and dynamics (F-actin labeled by Phalloidin), and phosphorylation of FAK (pFAK; activated focal adhesion kinase) were used as markers for cell migration. As readout for proliferation Ki67 expression was used. Antibodies against P-cadherin and EDAR (both red) were used to differentiate HF placodes. Arrowheads indicate Ki67 expression in HF placodes; dashed line delineates dermal-epidermal boundaries. Blue, nuclear DAPI staining. Scale bars: 20  $\mu$ m.

these genes contains a single NF- $\kappa$ B-binding site that was verified by ChIP (Fig. 2B; data not shown). Although we observed *Sox9* mRNA expression in suprabasal cells of primary HF placodes at E14.5 (Fig. S3C), SOX9 protein expression is not detected prior to E15.5 and does not play a role in HF induction and early morphogenesis, instead being required for formation and maintenance of early and adult bulge stem cells (Kadaja et al., 2014; Nowak et al., 2008; Vidal et al., 2005). We therefore focused on LHX2, as LHX2 protein was readily detected in control HF placodes, was congruent with NF- $\kappa$ B activity, and was absent in the epithelium of *ΔN* embryos at E14.5 (Fig. 2C).

To examine the precise role of LHX2 in HF morphogenesis, we examined primary guard hair placode formation in *Lhx2* knockout (*Lhx2*-KO) embryos at E14.5 and E15.5 compared with control littermates. A previous analysis of *Lhx2*-KO embryos revealed a 40% reduction of developing placodes at E16.5, when secondary HF induction sets in (Rhee et al., 2006). Similarly to *ΔN* embryos, *Lhx2*-KO embryos initiated primary HF pre-placode generation at E14.5 (Fig. 2D) (Schmidt-Ullrich et al., 2006; Zhang et al., 2009a). However, subsequent placode formation went on to stage 1, when most placodes seemed to be arrested (Fig. 2D). Direct LHX2 target genes that are involved in cell adhesion and cytoskeletal dynamics in the HF stem cell niche suggest a possible role for LHX2 in directed cell growth (Folgueras et al., 2013). In line with this, qRT-PCR showed that mRNA expression of genes involved in cell migration, such as the previously identified LHX2 target gene *Nrp1* (Folgueras et al., 2013) as well as the novel NF- $\kappa$ B-regulated genes *Nrp2* and *Prokr2*, were markedly downregulated in the epidermis of *Lhx2*-KO embryos at E14.5 (Fig. 2E). This was further supported by the lack of *in vivo* mRNA expression of *Nrp2* and *Prokr2* in placodes of *Lhx2*-KO embryos compared with controls at E14.5 (Fig. 2F). Again, a possible contamination of dermal cells in purified epidermal cell samples of *Lhx2*-KOs and controls was ruled out by analyzing mRNA expression of *Bmp4*, *Colla1*, *Irx1* and *Ngfr* (Fig. S2B). However, expression of *Nrp2* mRNA was conserved in the dermal condensate, indicating that *Nrp2* expression is differentially regulated in HF

placodes and dermal condensates (Fig. 2C,F). Notably, both *Nrp2* and *Prokr2* genes have potential NF- $\kappa$ B- and LHX2-binding sites in their promoter regions (Table S3), suggesting that these genes might be regulated synergistically by NF- $\kappa$ B and downstream LHX2.

#### ***Lhx2*-KO and *ΔN* mice display cell migratory and proliferative defects in down-growing primary HF placodes**

To explore further whether NF- $\kappa$ B and LHX2 cooperate in regulating directed placode keratinocyte migration and proliferation, we examined staining for F-actin (filamentous actin), phospho-FAK (pFAK; activated focal adhesion kinase) and Ki67 (also known as MKI67) on skin sections at E14.5 (Fig. 3). FAK (also known as PTK2), a non-receptor tyrosine kinase, regulates focal cell adhesion and directed migration, as well as polarity and proliferation (Frame et al., 2010; Schaller, 2010). FAK is stimulated by growth factors, such as platelet-derived growth factor and epidermal growth factor, and by integrin-ECM interactions, which lead to activation of FAK by phosphorylation (Sieg et al., 2000). FAK is essential for embryonic development and also plays an important role in epithelial oncogenesis (reviewed by Sulzmaier et al., 2014). Moreover, mice deficient in epidermal FAK lack proper HF down-growth and display hair cycle defects (Essayem et al., 2006; Schober et al., 2007). F-actin staining is also typically enhanced during directed cell migration. As expected, primary HF placodes of controls displayed pFAK and F-actin staining in the proximal placode border adjacent to the dermal condensate at E14.5 (Fig. 3). However, F-actin and pFAK were absent in the epithelium of *Lhx2*-KOs and *ΔN* embryos (Fig. 3). The proliferation marker Ki67 was also expressed in HF placodes of controls but was not detected in *Lhx2*-KO or *ΔN* embryos at E14.5 (Fig. 3). These data strongly suggest that NF- $\kappa$ B and downstream LHX2 are required to generate the appropriate environment for primary HF placode keratinocytes to proliferate and migrate into the underlying dermis.

#### ***Lhx2*-KO and *ΔN* mice show impaired TGF $\beta$ signaling and lack of E-cadherin downregulation**

In order to allow placode down-growth, cells at the very proximal border of the HF placode have to undergo a number of changes, including loss of cell adhesion. This involves local downregulation of the epithelial cadherin E-cadherin (cadherin 1), which forms the transmembrane core of adherens junctions (AJ) (Jamora et al., 2003, 2005). The TGF $\beta$  family of signaling molecules controls cell-cell interactions, cell migration and proliferation. In particular, TGF $\beta$ 2 promotes HF morphogenesis by inducing expression of the transcriptional repressor Snail (SNAI1) and mitogen-activated protein kinase activity, resulting in local E-cadherin downregulation (Jamora et al., 2005). Mice lacking TGF $\beta$ 2 activity display a delay in HF development and a 50% reduction in the numbers of follicles that form (Foitzik et al., 1999; Jamora et al., 2005). These studies only examined secondary HF development, which is independent of EDA-A1/EDAR/NF- $\kappa$ B signaling (Schmidt-Ullrich et al., 2001, 2006). During primary HF placode growth, E-cadherin downregulation must be independent of Snail because we did not detect any *Snai1* expression in our gene profiling analysis (Table S1), and a previous publication only revealed Snail protein expression at E16.5 (Jamora et al., 2005). By contrast *Snai3* was upregulated (1.6 $\times$ ) in primary hair placodes compared with interfollicular epidermis at E14.5 (Table S1), suggesting that it might substitute for Snail in primary hair placode growth.

Interestingly, *Tgfb2*-KO mice have a HF developmental phenotype that is very similar to that of *Lhx2*-KO mice (data not

shown; Fig. 4) (Foitzik et al., 1999). This prompted us to ask whether TGF $\beta$  signaling is affected in *Lhx2*-KO and  $\Delta N$  embryonic skin at E14.5. In control embryos, TGF $\beta$ 2 protein expression was detected in the suprabasal layer of the epidermis, in the entire placode border adjacent to the dermis and in the dermal condensate, the future dermal papilla (Fig. 4A, upper panels) (Jamora et al., 2005). Phospho-SMAD2 (pSMAD2) expression, which provides a sensitive read-out parameter for active TGF $\beta$  signaling, was observed in the entire epidermis, including HF placodes, and also in the dermal condensate of controls (Fig. 4A, upper panels). In *Lhx2*-KO embryos, TGF $\beta$ 2 protein was still expressed in the suprabasal epidermis, but pSMAD2 expression was reduced at this site compared with controls (Fig. 4A, upper panels). In HF placodes and dermal condensates of *Lhx2*-KO embryos, pSMAD2 expression was strongly reduced and TGF $\beta$ 2 protein expression was undetectable in both compartments at E14.5. Similarly to *Lhx2*-KOs,  $\Delta N$  embryos only expressed TGF $\beta$ 2 protein throughout the epidermis, but pSMAD2 expression was also strongly decreased (Fig. 4A, upper panels). However, qRT-PCR indicated that *Tgfb2* is

not a direct target gene of either NF- $\kappa$ B or LHX2 in epidermis or dermis (Fig. 1C; Fig. 4C; Table S2). Furthermore, the *Tgfb2* gene lacks binding sites for NF- $\kappa$ B and LHX2 (Table S3). This suggests an indirect control of TGF $\beta$ 2 protein expression and/or activity by NF- $\kappa$ B and LHX2 in placodes and dermal condensate.

In line with the findings described above, E-cadherin expression was absent in proximal placode borders of controls at E14.5, but was readily detectable in placodes of *Lhx2*-KO embryos (Fig. 4A, lower panels). As expected, in  $\Delta N$  embryos E-cadherin expression was observed in the entire epidermis without local downregulation because primary HF placode formation is barely initiated and only reaches a rudimentary stage 0/1 (Fig. 4A, lower panels) (Schmidt-Ullrich et al., 2006; Zhang et al., 2009a). We also analyzed fibronectin 1 (*Fn1*) expression, which plays an important role in cell adhesion, migration and proliferation during embryonic development (Schwarzbauer and DeSimone, 2011). *Fn1* mRNA expression was upregulated in control placodes at E14.5 (Fig. 4B,D). By contrast, *Lhx2*-KO embryos revealed diminished *Fn1* mRNA expression and in  $\Delta N$  embryos *Fn1* was not detected

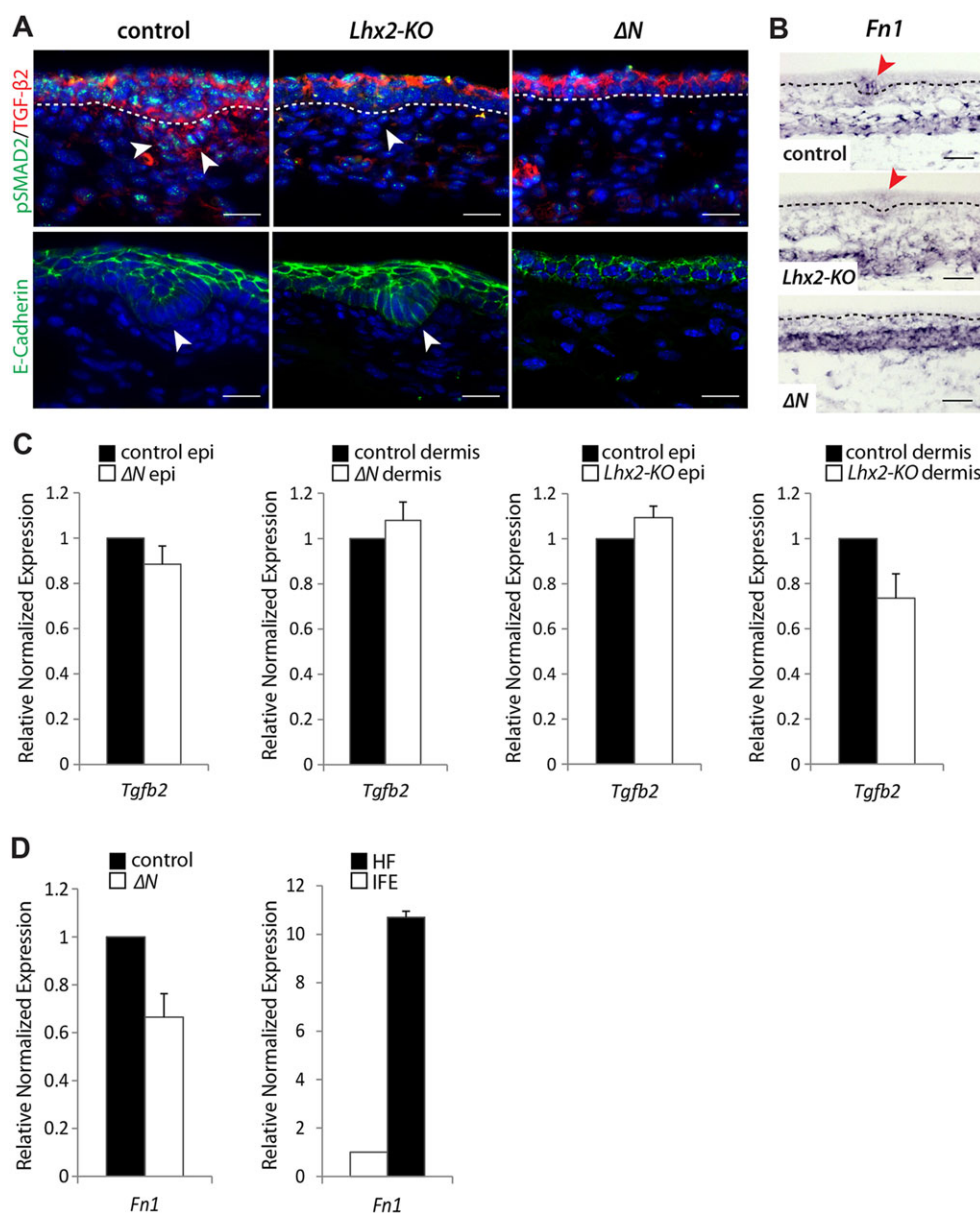


(Fig. 4B,D; see also Fig. 1C). Together, these findings suggest that delayed placode formation in *Lhx2*-KO mice and absent placode down-growth in  $\Delta N$  mice are caused in part by decreased TGF $\beta$ 2 signaling, failure of E-cadherin downregulation, and decreased Fn1 expression.

### Recombinant TGF $\beta$ 2 restores primary HF development in *Lhx2*-KO embryonic skin explants

As TGF $\beta$ 2 signaling appears to function downstream of LHX2 in primary HF placode formation, we investigated whether primary placode growth in *Lhx2*-KO mice could be rescued by treatment of cultured E14.5 skin explants with recombinant TGF $\beta$ 2. TGF $\beta$ 2 treatment of E14.5 skin explants from control mice slightly accelerated primary HF placode growth and expression of cell migration and proliferation markers or E-cadherin downregulation (Fig. S4A,B), consistent with previously published data (Foitzik et al., 1999). TGF $\beta$ 2-treated *Lhx2*-KO explants showed significantly increased formation of placodes at hair morphogenesis stages 1 and 2 after 24 h compared with untreated explants (Fig. 5A). TGF $\beta$ 2 treatment of *Lhx2*-KO explants not only rescued and enhanced placode down-growth, but also restored TGF $\beta$  signaling, downregulation of E-cadherin and levels of the cell migration and proliferation markers pFAK and Ki67 in HF placodes (Fig. 5B). Thus, TGF $\beta$ 2 activation acts downstream of LHX2 to promote transient E-cadherin downregulation. By contrast, treatment of  $\Delta N$  skin explant cultures with recombinant TGF $\beta$ 2 did not rescue HF development (Fig. S4A). This indicates that additional NF- $\kappa$ B targets, probably including growth regulators such as SHH, and/or physiological processes such as ECM remodeling (see above) are required downstream of NF- $\kappa$ B activity and cannot be compensated for by addition of TGF $\beta$  alone (Mill et al., 2003; Schmidt-Ullrich et al., 2006; St-Jacques et al., 1998; Zhang et al., 2009a).

### DISCUSSION

Here, we identified a novel NF- $\kappa$ B/LHX2/TGF $\beta$ 2 signaling axis that results in E-cadherin downregulation in primary HFs at early stages of their formation, an essential requirement for placode

down-growth (summarized in Fig. 6) (Jamora et al., 2003, 2005; Zhang et al., 2009a). Several EDA-A-dependent target genes have previously been identified and shown to function in HF development. These targets support a function for EDA-A1/EDAR/NF- $\kappa$ B signaling in placode patterning, WNT regulation and BMP suppression, but do not elucidate its role in intrinsic down-growth mechanisms (Bazzi et al., 2007; Cui et al., 2002, 2006; Fliniaux et al., 2008; Lefebvre et al., 2012; Mou et al., 2006; Pummila et al., 2007; Zhang et al., 2009a). Another downstream NF- $\kappa$ B target, SHH, promotes placode growth by upregulating cyclin D1 expression (see Fig. 1C) (Mill et al., 2003; Pummila et al., 2007; Schmidt-Ullrich et al., 2006). However, this occurs well after induction of EDA-A1/EDAR/NF- $\kappa$ B signaling, consistent with the later arrest of follicle development in *Shh*-deficient compared with NF- $\kappa$ B-inhibited mice (Chiang et al., 1999; Schmidt-Ullrich et al., 2006; St-Jacques et al., 1998). In the current study, we therefore sought to identify NF- $\kappa$ B-dependent factors that are specifically required to establish the appropriate conditions for placode down-growth beyond initiation. Our data confirm an essential role for EDA-A1/EDAR/NF- $\kappa$ B signaling in preparing primary hair pre-placodes for down-growth and identify several novel NF- $\kappa$ B target genes. Importantly, we identified the LIM homeobox transcription factor LHX2 as a crucial new NF- $\kappa$ B-controlled gene that contributes to providing the proper conditions for placode down-growth primarily by activation of TGF $\beta$ 2 signaling, a known hair placode growth inducer (summarized in Fig. 6) (Foitzik et al., 1999; Jamora et al., 2005).

We further show that NF- $\kappa$ B regulates genes involved in ECM remodeling (*Frem1*, *Mmp9*, *Tnc*), cell migration (*Nrp2*, *Prokr2*, *Cd74*) and adhesion (*Ncam1*, *Madcam1*) in primary hair placodes at E14.5. We have previously observed loss of structural organization at sites of placode induction when NF- $\kappa$ B activity is suppressed (Schmidt-Ullrich et al., 2006). This might be due in part to reorganization of the epidermis (Schmidt-Ullrich et al., 2006). The characteristic structural organization of epidermal keratinocytes and of the underlying dermal condensate at sites of placode formation is most likely an important prerequisite for

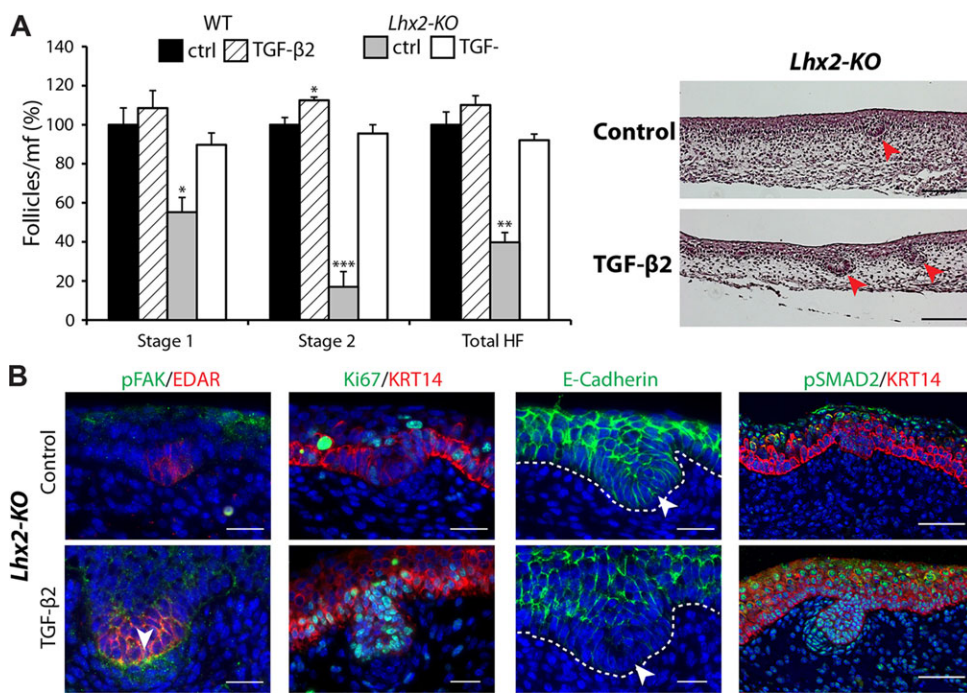


**Fig. 5. Treatment of *Lhx2*-KO embryonic skin explants with TGF $\beta$ 2 rescued proper primary HF development.** (A) Embryonic skin explants of  $n=3$  E14.5 control or *Lhx2*-KO mice were either left untreated (ctrl) or treated with recombinant TGF $\beta$ 2 (100 ng/ml) for 24 h. Skin samples were stained with H&E (right), and follicles were quantified as percentage relative to the number of follicles per microscopic field in the control group (left). Statistical analyses were performed using two-tailed unpaired t-test. Data were pooled from three biological replicates and presented as mean $\pm$ s.e.m. \* $P<0.05$ ; \*\* $P<0.01$ ; \*\*\* $P<0.001$ . Arrowheads indicate HF placodes. Scale bars: 100  $\mu$ m. (B) Immunostaining on *Lhx2*-KO explants treated with recombinant TGF $\beta$ 2 or left untreated (control) using antibodies against pFAK, EDAR, Ki67, KRT14, E-cadherin and pSMAD2. Arrowheads indicate pFAK and the presence or absence of E-cadherin expression in the HF placode border; dashed line delineates dermal-epidermal boundaries. Blue, nuclear DAPI staining. Scale bars: 20  $\mu$ m (pFAK, Ki67, E-cadherin); 50  $\mu$ m (pSMAD2).

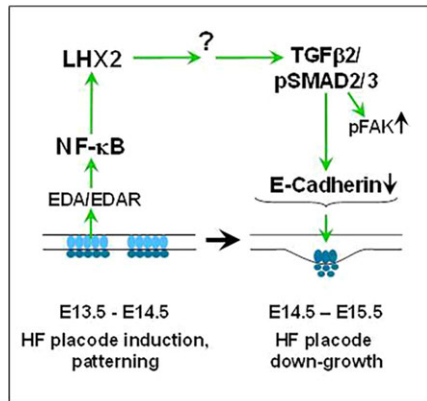


**Fig. 6. Model for primary placode down-growth involving NF-κB signaling.** We show here that LHX2 expression is directly regulated by EDA-A1/EDAR/NF-κB signaling, as NF-κB activity in primary placodes depends on EDA-A1/EDAR (Schmidt-Ullrich et al., 2006). By an as yet unknown mechanism LHX2 activates TGFβ2 signaling in primary HF placodes, which results in phosphorylation of FAK (pFAK), and, importantly, in downregulation of E-cadherin expression. Together, these results introduce a novel NF-κB/LHX2/TGFβ2 signaling axis that is required for establishing the proper conditions for placode down-growth, and might also be relevant for other epithelial-mesenchymal tissue interactions, for epithelial-mesenchymal transition or for tumor growth.

subsequent down-growth. It has also recently been suggested that EDA-A1/EDAR/NF-κB signaling is involved in modulating cell motility and placodal fate decisions resulting in early placode formation prior to down-growth, as mice with forced epidermal EDA-A1 expression displayed increased cell motility in the interfollicular epidermis and in future areas of HF formation (Ahtiainen et al., 2014). However, excess EDA-A1 expression generally results in premature and aberrant placode formation and, therefore, might not reflect the physiological role of endogenous EDA-A1 signaling in hair placode induction (Ahtiainen et al., 2014; Mustonen et al., 2003). Our detailed NF-κB-dependent gene signature in hair placodes supports a mandatory role for NF-κB signaling in ECM remodeling and cell migration and is consistent with our previous findings that NF-κB is required for placode pattern refinement and down-growth rather than rudimentary pre-placode formation and hair fate decisions, which are both dependent on canonical WNT signaling (Andl et al., 2002; Schmidt-Ullrich et al., 2006; Zhang et al., 2009a). Overall, our study illuminates a role for NF-κB in primary HF development that extends well beyond the previously described functions in terms of molecular controls in tissue remodeling, and might be relevant for understanding other epithelial-mesenchymal tissue interaction systems, such as those that occur in tumor growth.

After completion of our studies, an RNA-seq-based transcriptome of HF progenitors was published (Sennett et al., 2015) (see also <http://hair-gel.net/>). This useful resource confirms our findings regarding placode-specific expression of *Lhx2*, *Dkk4*, *Foxi3*, *Shh*, *Tnfaip*, *Wnt10b*, *Fgf20* and *Ascl4*. However, our *in situ* hybridization and qPCR studies revealed several inconsistencies, for instance regarding the location of *Fn1*, *Prokr2*, *Sox9*, *Nrp2*, *Frem1*, *Ncam1* and *Trps1* expression. The RNA-seq data of Sennett et al. indicate exclusive expression of these genes in the dermal compartment; however, our *in situ* hybridization and qPCR studies reveal that *Sox9*, *Prokr* and *Fn1* expression is confined to the hair placode, whereas *Nrp2*, *Frem1*, *Ncam1* and *Trps1* are expressed in both placode and dermal condensate (Fig. 1D,E; Fig. 2E,F; Fig. 4B; Fig. S3A-C). These discrepancies highlight the need to verify gene

expression patterns inferred from FACS analyses and transcriptional profiling using independent approaches.

Our data suggest that EDA-A1/EDAR/NF-κB controls primary placode down-growth at various levels, including ECM remodeling, and downstream expression of LHX2, which leads to activation of TGFβ2 signaling and subsequent E-cadherin downregulation (Fig. 6). In terms of hair placode growth delay, *Lhx2*-KO mice strongly resemble mice deficient in *Tgfb2* expression (Fig. 2) (Foitzik et al., 1999), and, similarly to *Tgfb2*-KOs (Jamora et al., 2005), E-cadherin downregulation was absent in stage 1 placodes of *Lhx2*-KO embryos at E14.5. The importance of E-cadherin downregulation for hair placode down-growth, which is dependent on TGFβ2 signaling, was demonstrated previously using mice with forced epidermal E-cadherin expression in which placode growth was totally blocked (Jamora et al., 2003, 2005). Although neither NF-κB nor LHX2 appear to control expression of the *Tgfb2* gene or components of the pathway (Fig. 1; Fig. 4C,D; Table S1) (Folgueras et al., 2013), activation of TGFβ2 signaling is downstream of both transcription factors and directly or indirectly depends on the transcriptional activity of LHX2. As almost all cell types express TGFβ receptors, TGFβ activation is tightly controlled. The TGFβ protein is produced as a latent inactive form that is mainly activated by binding to integrins (Worthington et al., 2011). It is thus conceivable that NF-κB and particularly LHX2 are indirectly responsible for the release of TGFβ2 from its latent inactive form. Initiation of placode down-growth leads to changes in the ECM at the proximal placode border. These changes are likely to be controlled by NF-κB and downstream LHX2 (see above) and may make local integrins available for binding to latent TGFβ complexes. Another reason for lack of TGFβ2 activity in *ΔN* and *Lhx2*-KO mice might be loss of *Nrp2* (neuropilin 2) expression in hair placodes of both mouse models. It was recently shown that neuropilins can activate the latent TGFβ complex (Glinka et al., 2011). Furthermore, neuropilins can act as co-receptors for TGFβ receptors and increase the response to latent and active TGFβ (Glinka et al., 2011). In *Lhx2*-KO mice, *Nrp2* mRNA expression was absent in the epidermis; however, it was still expressed in the dermal condensate, which may be sufficient to induce TGFβ signaling and placode down-growth when *Lhx2*-KO skin explants are treated with recombinant TGFβ2. Further investigation of the mechanisms by which NF-κB functions to mediate local changes in cell adhesion and ECM modulation in placode down-growth will be highly interesting in light of the important roles of NF-κB in tumor growth.

In mature follicles, LHX2 controls HF stem cell maintenance and proliferation by regulating cytoskeletal organization, polarity and cell adhesion within the niche (Folgueras et al., 2013; Mardaryev et al., 2011; Rhee et al., 2006). Placode growth also involves changes in cell adhesion, polarity and proliferation and we show that *Lhx2*-KO mice have delayed primary hair placode growth. Thus, in addition to its role in promoting TGFβ2 signaling, LHX2 might have some analogous functions in HF stem cell maintenance and in early primary placode down-growth. Exploring the molecular connections between embryonic HF precursors and adult stem cells will be a fascinating area for future studies.

## MATERIALS AND METHODS

### Generation of transgenic mice and animal experiments

All aspects of animal care and experimental protocols were approved by the Berlin Animal Review Board (Reg. G 0261/02, G 0077/08, G 0082/13 and X 9013/11). The EGFP cDNA was cloned immediately downstream of an artificial NF-κB-responsive promoter, which has been described previously

(Schmidt-Ullrich et al., 1996). The construct was linearized, purified and used for pronuclear microinjection to generate *B6-Tg(κ-EGFP)3Pt/Rsu* mice (here referred to as *κ-EGFP*). Pre-existing mouse strains used for this study have been described earlier: *129;129P2-ctmnb1tm(NFKBIAΔN)1Rsu* ( $\Delta N$ ) (Schmidt-Ullrich et al., 2001), *B6-Lhx2<sup>tm1Hwe</sup>* (*Lhx2* knockout mice, here referred to as *Lhx2*-KO, were kindly provided by H. Westphal) (Porter et al., 1997) and *B6CBACa-A<sup>w/J</sup>/A-Ta* (*tabby, ta/ta*) (*Eda-A1*-mutant mice, kindly provided by I. Thesleff) (Falconer, 1952). Mice and embryos were genotyped by PCR of genomic DNA. Heterozygous *Lhx2*-KO mice were crossbred to obtain homozygous mutants, which were collected before E16.5.

### Isolation of primary placode keratinocytes by flow cytometry

Back skin from E14.5 *κ-EGFP* embryos was dissected and treated overnight with dispase (BD Biosciences; 2.5 units/ml) at 4°C, which selectively separated the epidermis with primary placodes from the underlying dermis. The epidermal fraction was treated with 10 mM EDTA, and cell suspensions were subsequently strained (35-μm pores; BD Biosciences). Further purification of placode keratinocytes was performed using a FACS Aria III system, equipped with FACS DiVa software (BD Biosciences). Cells were gated for single events and viability, and then sorted by EGFP expression. Purity of the sorted placode keratinocyte population was determined by post-sort FACS analysis and typically exceeded 95% (Fig. S1). Back skin from E14.5 *κ-EGFP* embryos of various different litters was prepared this way and pooled for five independent microarray experiments.

### Microarray and qRT-PCR

Total RNA from either epidermal keratinocytes of five control or five  $\Delta N$  embryos at E14.5, or of FACS-purified EGFP-positive (placode) or EGFP-negative (IFE) epidermal keratinocytes from *κ-EGFP* embryos at E14.5 (see above) was isolated using the Absolutely RNA Microprep Kit (Agilent Technologies) and then processed with the WT Expression Kit (Ambion) and the WT Terminal Labeling and Hybridization Kit (Affymetrix). Processed RNA was hybridized to the Mouse Gene 1.0 ST Array (Affymetrix). Five biological replicates for each sample were analyzed statistically with the multi-factor ANOVA test using Partek Genomic Suites software (Partek). The complete microarray data are listed in Table S1. For quantitative real-time PCR (qRT-PCR), total RNA was used to generate cDNA by means of the iScript cDNA Synthesis Kit (Bio-Rad). qRT-PCR primers were designed using Primer3 software (see Table S2). See supplementary Materials and Methods for primer sequences. Reactions were performed in triplicate using the GoTaq qPCR Master Mix (Promega) and a CFX 96 real-time PCR detection system (Bio-Rad). Differences between samples were calculated using the CFX Manager software (Bio-Rad) based on the  $\Delta\Delta Ct$  equitation method, and were normalized to three house-keeping genes (*Actb*, *Gapdh* and *Hmbs*). Statistical significance was estimated using unpaired Student's *t*-test.

### Histology, immunofluorescence and *in situ* hybridization

Back skin samples were fixed in 4% paraformaldehyde/MEM or in Bouin's fixative overnight at 4°C, and were either directly embedded in Tissue Tek O.C.T. or dehydrated and paraffin-embedded. Routine Hematoxylin and Eosin (H&E) staining was performed for morphological evaluation. The progress of HF development was assessed by morphometry using the classification of HF stages by Hardy (1992) and Paus et al. (1999). Cryosections were used for cytoskeleton staining with Phalloidin coupled to Alexa Fluor 488 (Life Technologies, 1:100). Immunofluorescence and *in situ* hybridization on paraffin sections were performed as described previously (Zhang et al., 2009a). Antibodies and dilutions used were: rat anti-P-cadherin (Invitrogen, 13-2000Z; 1:400); chicken anti-EGFP (Abcam, ab13970; 1:1600); goat anti-LHX2 (Santa Cruz Biotechnology, Sc-19344; 1:400); rabbit and chicken anti-KRT14 (Convance, AF64 and CK14; 1:2000); goat anti-EDAR (R&D Systems, AF745; 1:200); rabbit anti-pSMAD2 (Cell Signaling, #3101; 1:400); rabbit anti-phospho-FAK (Y397) (Santa Cruz, sc-11765R; 1:400); rabbit anti-Ki67 (Abcam, ab15580; 1:400); mouse anti-E-cadherin (BD Biosciences, #610181; 1:100); mouse anti-TGFβ2 (Abcam, ab36495; 1:100); digoxigenin-conjugated sheep anti-AP Fab fragments (Roche, #11093274910; 1:1000).

Probe sequences used for *in situ* hybridization are provided in the supplementary Materials and Methods. Images were obtained by a conventional or confocal Zeiss microscope.

### Chromatin immunoprecipitation (ChIP)

One million EGFP-positive (placode) or EGFP-negative (IFE) epidermal keratinocytes from E14.5 *κ-EGFP* embryos were fixed in 1% formaldehyde for 10 min at room temperature. Subsequent cell lysis, sonification and ChIP assays were performed using the MAGnify Chromatin Immunoprecipitation System (Invitrogen). For each immunoprecipitation, cells were incubated with 6 μg rabbit anti-NF-κB p65 (RelA) antibody (Santa Cruz, sc-372 X). qRT-PCR was then performed to visualize specific enrichment of potential NF-κB binding regions. Ct values of the region of interest and a control region (transcription start site of *Gapdh*) were measured in the input and ChIP sample, and  $\Delta Ct$  values were calculated. Three replicates were measured and mean ± s.e.m. was calculated. Statistical analysis was performed using unpaired Student's *t*-test. Primers are listed in supplementary Materials and Methods.

### Embryonic skin culture

Back skin explants from *Lhx2*-KO and control littermates were collected at E14.5, transferred onto 0.1 μm PVDF membranes (Millipore) and cultured using Advanced DMEM:F12 (Gibco) supplemented with 0.5 mM L-glutamine and 100 units/ml penicillin/streptomycin. Skins were kept in a floating culture. Explants were either treated with 100 ng/ml human recombinant TGFβ2 (PeproTech) or left untreated. After 24 h, explants were harvested and prepared for paraffin embedding (see above). Progression of HF development was monitored in three independent biological replicates. For each replicate, the number of placode and germ stage follicles per microscopic field (100×) was calculated in 30 H&E-stained sections. *P*-values were calculated using unpaired Student's *t*-test.

### Acknowledgements

We thank Sandra Herms, Inge Krahm, Doris Lange, Vivian Schulz, Lisa Spatt and Sarah Ugowski for excellent technical help and animal welfare and breeding; Heiner Westphal for *Lhx2*-KO mice; Irma Thesleff for *Ta/Ta* mice; Ronald Naumann for transgenic mouse production; and Hans-Peter Rahn (FACS) and Gabriele Born (MCF core facility, MDC) for technical assistance.

### Competing interests

The authors declare no competing or financial interests.

### Author contributions

P.T. designed and performed the experiments, and analyzed the data. R.P. designed experiments, analyzed the data and edited the manuscript. S.E.M. analyzed the data and edited the manuscript. C.S. analyzed the data and edited the manuscript. R.S.-U. oversaw the entire project, designed experiments, analyzed the data and wrote the paper.

### Funding

This work was funded by grants from the German Research Foundation (Deutsche Forschungsgemeinschaft, DFG) [SCHM 855/3-3 to R.S.-U. and PA 345/13-3 to R.P.].

### Data availability

Microarray data have been deposited in ArrayExpress under accession numbers E-MTAB-4534 (gene expression in total epidermis of E14.5 mouse embryos with blocked NF-κB pathway) and E-MTAB-4535 (primary hair placode profiling).

### Supplementary information

Supplementary information available online at <http://dev.biologists.org/lookup/suppl/doi:10.1242/dev.130898/-DC1>

### References

- Ahtiainen, L., Lefebvre, S., Lindfors, P. H., Renvoisé, E., Shirokova, V., Vartiainen, M. K., Thesleff, I. and Mikkola, M. L. (2014). Directional cell migration, but not proliferation, drives hair placode morphogenesis. *Dev. Cell* **28**, 588–602.
- Andl, T., Reddy, S. T., Gaddapara, T. and Millar, S. E. (2002). WNT signals are required for the initiation of hair follicle development. *Dev. Cell* **2**, 643–653.
- Bazzi, H., Fantauzzo, K. A., Richardson, G. D., Jahoda, C. A. B. and Christiano, A. M. (2007). The Wnt inhibitor, Dickkopf 4, is induced by canonical Wnt signaling during ectodermal appendage morphogenesis. *Dev. Biol.* **305**, 498–507.

- Biggs, L. C. and Mikkola, M. L.** (2014). Early inductive events in ectodermal appendage morphogenesis. *Semin. Cell Dev. Biol.* **25-26**, 11-21.
- Botchkarev, V. A., Botchkareva, N. V., Roth, W., Nakamura, M., Chen, L.-H., Herzog, W., Lindner, G., McMahon, J. A., Peters, C., Lauster, R. et al.** (1999). Noggin is a mesenchymally derived stimulator of hair-follicle induction. *Nat. Cell Biol.* **1**, 158-164.
- Botchkareva, N. V., Botchkarev, V. A., Chen, L.-H., Lindner, G. and Paus, R.** (1999). A role for p75 neurotrophin receptor in the control of hair follicle morphogenesis. *Dev. Biol.* **216**, 135-153.
- Bulchand, S., Grove, E. A., Porter, F. D. and Tole, S.** (2001). LIM-homeodomain gene Lhx2 regulates the formation of the cortical hem. *Mech. Dev.* **100**, 165-175.
- Chen, D., Jarrell, A., Guo, C., Lang, R. and Atit, R.** (2012). Dermal beta-catenin activity in response to epidermal Wnt ligands is required for fibroblast proliferation and hair follicle initiation. *Development* **139**, 1522-1533.
- Chiang, C., Swan, R. Z., Grachchouk, M., Bolinger, M., Litingtung, Y., Robertson, E. K., Cooper, M. K., Gaffield, W., Westphal, H., Beachy, P. A. et al.** (1999). Essential role for Sonic hedgehog during hair follicle morphogenesis. *Dev. Biol.* **205**, 1-9.
- Cui, C.-Y., Durmowicz, M., Tanaka, T. S., Hartung, A. J., Tezuka, T., Hashimoto, K., Ko, M. S. H., Srivastava, A. K. and Schlessinger, D.** (2002). EDA targets revealed by skin gene expression profiles of wild-type, Tabby and Tabby EDA-A1 transgenic mice. *Hum. Mol. Genet.* **11**, 1763-1773.
- Cui, C.-Y., Hashimoto, T., Grivennikov, S. I., Piao, Y., Nedospasov, S. A. and Schlessinger, D.** (2006). Ectodysplasin regulates the lymphotoxin-beta pathway for hair differentiation. *Proc. Natl. Acad. Sci. USA* **103**, 9142-9147.
- de Oliveira, K. A., Kaergel, E., Heinig, M., Fontaine, J. F., Patone, G., Muro, E. M., Mathas, S., Hummel, M., Andrade-Navarro, M. A., Hübsner, N. and Scheidererit, C.** (2016). A roadmap of constitutive NF- $\kappa$ B activity in Hodgkin lymphoma: dominant roles of p50 and p52 revealed by genome-wide analyses. *Genome Med.* **8**, 28. doi:10.1186/s13073-016-0280-5.
- Essayem, S., Kovacic-Milivojevic, B., Baumbusch, C., McDonagh, S., Dolganov, G., Howerton, K., Larocque, N., Mauro, T., Ramirez, A., Ramos, D. M. et al.** (2006). Hair cycle and wound healing in mice with a keratinocyte-restricted deletion of FAK. *Oncogene* **25**, 1081-1089.
- Falconer, D. S.** (1952). A totally sex-linked gene in the house mouse. *Nature* **169**, 664-665.
- Fantauzzo, K. A., Bazzi, H., Jahoda, C. A. B. and Christiano, A. M.** (2008a). Dynamic expression of the zinc-finger transcription factor Trps1 during hair follicle morphogenesis and cycling. *Gene Expr. Patterns* **8**, 51-57.
- Fantauzzo, K. A., Tadin-Strappas, M., You, Y., Mentzer, S. E., Baumeister, F. A. M., Cianfarani, S., Van Maldergem, L., Warburton, D., Sundberg, J. P. and Christiano, A. M.** (2008b). A position effect on TRPS1 is associated with Ambras syndrome in humans and the Koala phenotype in mice. *Hum. Mol. Genet.* **17**, 3539-3551.
- Fliniaux, I., Mikkola, M. L., Lefebvre, S. and Thesleff, I.** (2008). Identification of dkk4 as a target of Eda-A1/Edar pathway reveals an unexpected role of ectodysplasin as inhibitor of Wnt signalling in ectodermal placodes. *Dev. Biol.* **320**, 60-71.
- Foitzik, K., Paus, R., Doetschman, T. and Dotto, G. P.** (1999). The TGF-beta2 isoform is both a required and sufficient inducer of murine hair follicle morphogenesis. *Dev. Biol.* **212**, 278-289.
- Folgueras, A. R., Guo, X., Pasolli, H. A., Stokes, N., Polak, L., Zheng, D. and Fuchs, E.** (2013). Architectural niche organization by LHX2 is linked to hair follicle stem cell function. *Cell Stem Cell* **13**, 314-327.
- Frame, M. C., Patel, H., Serrels, B., Lietha, D. and Eck, M. J.** (2010). The FERM domain: organizing the structure and function of FAK. *Nat. Rev. Mol. Cell Biol.* **11**, 802-814.
- Fuchs, E.** (2007). Scratching the surface of skin development. *Nature* **445**, 834-842.
- Glinka, Y., Stoilova, S., Mohammed, N. and Prud'homme, G. J.** (2011). Neuropilin-1 exerts co-receptor function for TGF-beta-1 on the membrane of cancer cells and enhances responses to both latent and active TGF-beta. *Carcinogenesis* **32**, 613-621.
- Hardy, M. H.** (1992). The secret life of the hair follicle. *Trends Genet.* **8**, 55-61.
- Headon, D. J. and Overbeek, P. A.** (1999). Involvement of a novel Tnf receptor homologue in hair follicle induction. *Nat. Genet.* **22**, 370-374.
- Hirota, J. and Mombaerts, P.** (2004). The LIM-homeodomain protein Lhx2 is required for complete development of mouse olfactory sensory neurons. *Proc. Natl. Acad. Sci. USA* **101**, 8751-8755.
- Jamora, C., DasGupta, R., Kocieniewski, P. and Fuchs, E.** (2003). Links between signal transduction, transcription and adhesion in epithelial bud development. *Nature* **422**, 317-322.
- Jamora, C., Lee, P., Kocieniewski, P., Azhar, M., Hosokawa, R., Chai, Y. and Fuchs, E.** (2005). A signaling pathway involving TGF-beta2 and snail in hair follicle morphogenesis. *PLoS Biol.* **3**, e11.
- Jiang, T.-X., Widelitz, R. B., Shen, W.-M., Will, P., Wu, D.-Y., Lin, C.-M., Jung, H.-S. and Chuong, C.-M.** (2004). Integument pattern formation involves genetic and epigenetic controls: feather arrays simulated by digital hormone models. *Int. J. Dev. Biol.* **48**, 117-135.
- Johnson, J.-L. F. A., Hall, T. E., Dyson, J. M., Sonntag, C., Ayers, K., Berger, S., Gautier, P., Mitchell, C., Hollway, G. E. and Currie, P. D.** (2012). Scube activity is necessary for Hedgehog signal transduction in vivo. *Dev. Biol.* **368**, 193-202.
- Kadaja, M., Keyes, B. E., Lin, M., Pasolli, H. A., Genander, M., Polak, L., Stokes, N., Zheng, D. and Fuchs, E.** (2014). SOX9: a stem cell transcriptional regulator of secreted niche signaling factors. *Genes Dev.* **28**, 328-341.
- Kere, J., Srivastava, A. K., Montonen, O., Zonana, J., Thomas, N., Ferguson, B., Munoz, F., Morgan, D., Clarke, A., Baybayan, P. et al.** (1996). X-linked anhidrotic (hypohidrotic) ectodermal dysplasia is caused by mutation in a novel transmembrane protein. *Nat. Genet.* **13**, 409-416.
- Kiso, M., Tanaka, S., Saba, R., Matsuda, S., Shimizu, A., Ohyama, M., Okano, H. J., Shiroishi, T., Okano, H. and Saga, Y.** (2009). The disruption of Sox21-mediated hair shaft cuticle differentiation causes cyclic alopecia in mice. *Proc. Natl. Acad. Sci. USA* **106**, 9292-9297.
- Kumar, A., Eby, M. T., Sinha, S., Jasmin, A. and Chaudhary, P. M.** (2001). The ectodermal dysplasia receptor activates the nuclear factor-kappaB, JNK, and cell death pathways and binds to ectodysplasin A. *J. Biol. Chem.* **276**, 2668-2677.
- Kunath, M., Lüdecke, H.-J. and Vortkamp, A.** (2002). Expression of Trps1 during mouse embryonic development. *Gene Expr. Patterns* **2**, 119-122.
- Laurikkala, J., Pispa, J., Jung, H. S., Nieminen, P., Mikkola, M., Wang, X., Saarilho-Kere, U., Galceran, J., Grosschedl, R. and Thesleff, I.** (2002). Regulation of hair follicle development by the TNF signal ectodysplasin and its receptor Edar. *Development* **129**, 2541-2553.
- Le Bail, O., Schmidt-Ullrich, R. and Israel, A.** (1993). Promoter analysis of the gene encoding the I kappa B-alpha/MAD3 inhibitor of NF-kappa B: positive regulation by members of the rel/NF-kappa B family. *EMBO J.* **12**, 5043-5049.
- Lefebvre, S., Fliniaux, I., Schneider, P. and Mikkola, M. L.** (2012). Identification of ectodysplasin target genes reveals the involvement of chemokines in hair development. *J. Invest. Dermatol.* **132**, 1094-1102.
- Lettice, L. A., Williamson, I., Wiltshire, J. H., Peluso, S., Devenney, P. S., Hill, A. E., Essafi, A., Hagman, J., Mort, R., Grimes, G. et al.** (2012). Opposing functions of the ETS factor family define Shh spatial expression in limb buds and underlie polydactyly. *Dev. Cell* **22**, 459-467.
- Malik, T. H., von Storchow, D., Bronson, R. T. and Shivdasani, R. A.** (2002). Deletion of the GATA domain of TRPS1 causes an absence of facial hair and provides new insights into the bone disorder in inherited tricho-rhino-phalangeal syndromes. *Mol. Cell. Biol.* **22**, 8592-8600.
- Mangale, V. S., Hirokawa, K. E., Satyaki, P. R. V., Gokulchandran, N., Chikibire, S., Subramanian, L., Shetty, A. S., Martynoga, B., Paul, J., Mai, M. V. et al.** (2008). Lhx2 selector activity specifies cortical identity and suppresses hippocampal organizer fate. *Science* **319**, 304-309.
- Mao, J., McGlenn, E., Huang, P., Tabin, C. J. and McMahon, A. P.** (2009). Fgf-dependent Etv4/5 activity is required for posterior restriction of Sonic Hedgehog and promoting outgrowth of the vertebrate limb. *Dev. Cell* **16**, 600-606.
- Mardarayev, A. N., Meier, N., Poterlowicz, K., Sharov, A. A., Sharova, T. Y., Ahmed, M. I., Rapisarda, V., Lewis, C., Fessing, M. Y., Ruenger, T. M. et al.** (2011). Lhx2 differentially regulates Sox9, Tcf4 and Lgr5 in hair follicle stem cells to promote epidermal regeneration after injury. *Development* **138**, 4843-4852.
- Mill, P., Mo, R., Fu, H., Grachchouk, M., Kim, P. C. W., Dlugosz, A. A. and Hui, C.-C.** (2003). Sonic hedgehog-dependent activation of Gli2 is essential for embryonic hair follicle development. *Genes Dev.* **17**, 282-294.
- Momeni, P., Glöckner, G., Schmidt, O., von Holtum, D., Albrecht, B., Gillessen-Kaesbach, G., Hennekom, R., Meinecke, P., Zabel, B., Rosenthal, A. et al.** (2000). Mutations in a new gene, encoding a zinc-finger protein, cause tricho-rhino-phalangeal syndrome type I. *Nat. Genet.* **24**, 71-74.
- Mou, C., Jackson, B., Schneider, P., Overbeek, P. A. and Headon, D. J.** (2006). Generation of the primary hair follicle pattern. *Proc. Natl. Acad. Sci. USA* **103**, 9075-9080.
- Mustonen, T., Pispa, J., Mikkola, M. L., Pummila, M., Kangas, A. T., Pakkasjärvi, L., Jaatinen, R. and Thesleff, I.** (2003). Stimulation of ectodermal organ development by Ectodysplasin-A1. *Dev. Biol.* **259**, 123-136.
- Nowak, J. A., Polak, L., Pasolli, H. A. and Fuchs, E.** (2008). Hair follicle stem cells are specified and function in early skin morphogenesis. *Cell Stem Cell* **3**, 33-43.
- Oro, A. E. and Scott, M. P.** (1998). Splitting hairs: dissecting roles of signaling systems in epidermal development. *Cell* **95**, 575-578.
- Paus, R., Muller-Rover, S., Van Der Veen, C., Maurer, M., Eichmuller, S., Ling, G., Hofmann, U., Foitzik, K., Mecklenburg, L. and Handjiski, B.** (1999). A comprehensive guide for the recognition and classification of distinct stages of hair follicle morphogenesis. *J. Invest. Dermatol.* **113**, 523-532.
- Porter, F. D., Drago, J., Xu, Y., Cheema, S. S., Wassif, C., Huang, S. P., Lee, E., Grinberg, A., Massalas, J. S., Bodine, D. et al.** (1997). Lhx2, a LIM homeobox gene, is required for eye, forebrain, and definitive erythrocyte development. *Development* **124**, 2935-2944.
- Pummila, M., Fliniaux, I., Jaatinen, R., James, M. J., Laurikkala, J., Schneider, P., Thesleff, I. and Mikkola, M. L.** (2007). Ectodysplasin has a dual role in ectodermal organogenesis: inhibition of Bmp activity and induction of Shh expression. *Development* **134**, 117-125.
- Rhee, H., Polak, L. and Fuchs, E.** (2006). Lhx2 maintains stem cell character in hair follicles. *Science* **312**, 1946-1949.

- Schaller, M. D.** (2010). Cellular functions of FAK kinases: insight into molecular mechanisms and novel functions. *J. Cell Sci.* **123**, 1007-1013.
- Schmidt-Ullrich, R. and Paus, R.** (2005). Molecular principles of hair follicle induction and morphogenesis. *Bioessays* **27**, 247-261.
- Schmidt-Ullrich, R., Memet, S., Lilienbaum, A., Feuillard, J., Raphael, M. and Israel, A.** (1996). NF-kappaB activity in transgenic mice: developmental regulation and tissue specificity. *Development* **122**, 2117-2128.
- Schmidt-Ullrich, R., Aebsicher, T., Hulskens, J., Birchmeier, W., Klemm, U. and Scheidereit, C.** (2001). Requirement of NF-kappaB/Rel for the development of hair follicles and other epidermal appendices. *Development* **128**, 3843-3853.
- Schmidt-Ullrich, R., Tobin, D. J., Lenhard, D., Schneider, P., Paus, R. and Scheidereit, C.** (2006). NF-kappaB transmits Eda A1/EdaR signalling to activate Shh and cyclin D1 expression, and controls post-initiation hair placode down growth. *Development* **133**, 1045-1057.
- Schneider, M. R., Schmidt-Ullrich, R. and Paus, R.** (2009). The hair follicle as a dynamic miniorgan. *Curr. Biol.* **19**, R132-R142.
- Schober, M., Raghavan, S., Nikolova, M., Polak, L., Pasolli, H. A., Beggs, H. E., Reichardt, L. F. and Fuchs, E.** (2007). Focal adhesion kinase modulates tension signaling to control actin and focal adhesion dynamics. *J. Cell Biol.* **176**, 667-680.
- Schwarzbauer, J. E. and DeSimone, D. W.** (2011). Fibronectins, their fibrillogenesis, and in vivo functions. *Cold Spring Harb. Perspect. Biol.* **3**, a005041.
- Sennett, R. and Rendl, M.** (2012). Mesenchymal–epithelial interactions during hair follicle morphogenesis and cycling. *Semin. Cell Dev. Biol.* **23**, 917-927.
- Sennett, R., Wang, Z., Rezza, A., Grisanti, L., Roitershtein, N., Sicchio, C., Mok, K. W., Heitman, N. J., Clavel, C., Ma'ayan, A. et al.** (2015). An integrated transcriptome atlas of embryonic hair follicle progenitors, their niche, and the developing skin. *Dev. Cell* **34**, 577-591.
- Shetty, A. S., Godbole, G., Maheshwari, U., Padmanabhan, H., Chaudhary, R., Muralidharan, B., Hou, P.-S., Monuki, E. S., Kuo, H.-C., Rema, V. et al.** (2013). Lhx2 regulates a cortex-specific mechanism for barrel formation. *Proc. Natl. Acad. Sci. USA* **110**, E4913-E4921.
- Shirokova, V., Jussila, M., Hytönen, M. K., Perälä, N., Drögemüller, C., Leeb, T., Lohi, H., Sainio, K., Thesleff, I. and Mikkola, M. L.** (2013). Expression of Foxi3 is regulated by ectodysplasin in skin appendage placodes. *Dev. Dyn.* **242**, 593-603.
- Sick, S., Reinker, S., Timmer, J. and Schlake, T.** (2006). WNT and DKK determine hair follicle spacing through a reaction-diffusion mechanism. *Science* **314**, 1447-1450.
- Sieg, D. J., Hauck, C. R., Ilic, D., Klingbeil, C. K., Schaefer, E., Damsky, C. H. and Schlaepfer, D. D.** (2000). FAK integrates growth-factor and integrin signals to promote cell migration. *Nat. Cell Biol.* **2**, 249-256.
- St-Jacques, B., Dassule, H. R., Karavanova, I., Botchkarev, V. A., Li, J., Danielian, P. S., McMahon, J. A., Lewis, P. M., Paus, R. and McMahon, A. P.** (1998). Sonic hedgehog signaling is essential for hair development. *Curr. Biol.* **8**, 1058-1069.
- Sulzmaier, F. J., Jean, C. and Schlaepfer, D. D.** (2014). FAK in cancer: mechanistic findings and clinical applications. *Nat. Rev. Cancer* **14**, 598-610.
- Takeuchi, M. and Baichwal, V. R.** (1995). Induction of the gene encoding mucosal vascular addressin cell adhesion molecule 1 by tumor necrosis factor alpha is mediated by NF-kappa B proteins. *Proc. Natl. Acad. Sci. USA* **92**, 3561-3565.
- Törnqvist, G., Sandberg, A., Häggglund, A.-C. and Carlsson, L.** (2010). Cyclic expression of lhx2 regulates hair formation. *PLoS Genet.* **6**, e1000904.
- Tsao, K.-C., Tu, C.-F., Lee, S.-J. and Yang, R.-B.** (2013). Zebrafish scube1 (signal peptide-CUB (complement protein C1r/C1s, Uegf, and Bmp1)-EGF (epidermal growth factor) domain-containing protein 1) is involved in primitive hematopoiesis. *J. Biol. Chem.* **288**, 5017-5026.
- Vidal, V. P. I., Chaboissier, M.-C., Lützkendorf, S., Cotsarelis, G., Mill, P., Hui, C.-C., Ortonne, N., Ortonne, J.-P. and Schedl, A.** (2005). Sox9 is essential for outer root sheath differentiation and the formation of the hair stem cell compartment. *Curr. Biol.* **15**, 1340-1351.
- Worthington, J. J., Klementowicz, J. E. and Travis, M. A.** (2011). TGFbeta: a sleeping giant awoken by integrins. *Trends Biochem. Sci.* **36**, 47-54.
- Yan, M., Wang, L.-C., Hymowitz, S. G., Schilbach, S., Lee, J., Goddard, A., de Vos, A. M., Gao, W.-Q. and Dixit, V. M.** (2000). Two-amino acid molecular switch in an epithelial morphogen that regulates binding to two distinct receptors. *Science* **290**, 523-527.
- Yoon, S., Woo, S. U., Kang, J. H., Kim, K., Shin, H.-J., Gwak, H.-S., Park, S. and Chwae, Y.-J.** (2012). NF-kappaB and STAT3 cooperatively induce IL6 in starved cancer cells. *Oncogene* **31**, 3467-3481.
- Yoshizaki, T., Sato, H., Furukawa, M. and Pagano, J. S.** (1998). The expression of matrix metalloproteinase 9 is enhanced by Epstein-Barr virus latent membrane protein 1. *Proc. Natl. Acad. Sci. USA* **95**, 3621-3626.
- Zhang, Y., Andl, T., Yang, S. H., Teta, M., Liu, F., Seykora, J. T., Tobias, J. W., Piccolo, S., Schmidt-Ullrich, R., Nagy, A. et al.** (2008). Activation of {beta}-catenin signaling programs embryonic epidermis to hair follicle fate. *Development* **135**, 2161-2172.
- Zhang, Y., Tomann, P., Andl, T., Gallant, N. M., Huelsken, J., Jerchow, B., Birchmeier, W., Paus, R., Piccolo, S., Mikkola, M. L. et al.** (2009a). Reciprocal requirements for EDA/EDAR/NF-kappaB and Wnt/beta-catenin signaling pathways in hair follicle induction. *Dev. Cell* **17**, 49-61.
- Zhang, Y., Verheyden, J. M., Hassell, J. A. and Sun, X.** (2009b). FGF-regulated Etv genes are essential for repressing Shh expression in mouse limb buds. *Dev. Cell* **16**, 607-613.

## Supplementary Materials and Methods

### In situ hybridization probes

In situ hybridization was carried out using the following mouse cDNA probe templates: pSport1-Fn1-31-38 (nt +4891 - +6157), pCMV-Sport6-Cd74 (IMAGE ID 2650401), pBSK-Prokr2-II (nt -275 - +741), pBSK-Nrp2-II (nt +1147 - +3503), pBSK-Gli1 and pBSK-Sox9 (kindly provided by T. Willnow), pCMV-Sport6.1-Frem1 (IMAGE ID 6510171), pCMV-Sport6.1-Mmp9 (IMAGE ID 6309245), pCMV- Sport6-Etv4 (IMAGE ID 4021693), pYX-Asc-Scube1 (IMAGE ID 6850999), pFLCI-Madcam1 (FANTOM Full Length cDNA clone 9430044H04), pGEM-Foxi3 (nt 3851 – 4461, GeneID: 232077), pGEM-Ascl4 (nt -180 – +785, GeneID:67341), pCR-BluntII-TOPO-Tnc (IMAGE ID 40099596), pCMV- Sport6-Pthlh (IMAGE ID 3594509), pYX-Asc-Tnfaip3 (IMAGE ID 6838303), pCR-BluntII-TOPO-Tsku (IMAGE-ID 40095311), pGEM-Ctgf (kindly provided by M. Mikkola), Bmp2 and Ptch1 (kindly provided by J. Huelsken).

### qRT-PCR primers

Reference genes :

mActb_RT_fwd sense:	5' TTACTGCTCTGGCTCCTAG 3'
mActb_RT_rev antisense:	5' CTCATCGTACTCCTGCTTG 3'
mGapdh_RT_fwd2 sense:	5' TGTGAACCACGAGAAATATGAC 3'
mGapdh_RT_rev2 antisense:	5' GTGATGGCATGGACTGTG 3'
mHmbs_RT_fwd sense:	5' CTGAAAGCCTTGTACCCCTG 3'
mHmbs_RT_rev antisense:	5' GCGTTTCTAGCTCCTTGG 3'

Target genes:

mAscl4_RT_fwd2 sense:	5' TAGCAGCATCCTAGCCCCACT 3'
mAscl4_RT_rev2 antisense:	5' ACTCGAACCAATGAAGGTG 3'
mBmp2_RT_fwd sense:	5' GCAGCTTCCATCACGAA 3'
mBmp2_RT_rev antisense:	5' TTCCTGTATCTGTTCCCG 3'
mBmp4_RT_fwd2 sense	5' GTAGTGCCATTGGAGCG 3'
mBmp4_RT_rev2 antisense	5' ATCAGCATTGGTTACCAGG 3'
mCd74_RT_fwd sense:	5' GAAATCTGCCAACCTGTG 3'
mCd74_RT_rev antisense:	5' GGTATGTTGCCGTACTT 3'
mColla1_RT_fwd1 sense	5' CTGCACGAGTCACACCGGAA 3'
mCoL1a1_RT_rev1 antisense	5' GGGAGGAAACCAGATTGGGG 3'
mCtgf_RT_fwd sense:	5' CCACCCGAGTTACCAATG 3'
mCtgf_RT_rev antisense:	5' TGGCGATTTAGGTGTCC 3'
mDkk4_RT_fwd sense:	5' AGCAGAGGAAAACAGACC 3'
mDkk4_RT_rev antisense:	5' CCACAGTCAGAGGTCTAAG 3'
mEdaR_RT_fwd2 sense:	5' GGATGTGTATGCCAACGTG 3'
mEdaR_RT_rev2 antisense:	5' GCCATGTTTCACGACCG 3'
mEtv4_RT_fwd sense:	5' ACCTCAGTCACTCCAAGAG 3'
mEtv4_RT_rev antisense:	5' GTTCCCTCTTGATCCTGGTG 3'
mEtv5_RT_fwd2 sense:	5' GCAGTTGTCAGATTTCA 3'
mEtv5_RT_rev2 antisense:	5' GGCACTTTCTCCATACTTAGC 3'
mFn1_RT_fwd sense:	5' GGAGAACAAAGACAGAGACAA 3'
mFn1_RT_rev antisense:	5' GGTGGATCTGTAGTCAGTG 3'
mFoxi3_RT_fwd sense:	5' AACTCCATCCGCCACAAC 3'
mFoxi3_RT_rev2 antisense:	5' CTTCCCACTCACTCTTAGTC 3'
mFrem1_RT_fwd sense:	5' ACCAGTTCACAGTATATGCC 3'
mFrem1_RT_rev antisense:	5' CCAGTTCTACCATGTGCC 3'
mGli1_RT_fwd2 sense:	5' TCAATCCAATGACTCCACC 3'
mGli1_RT_rev2 antisense:	5' GGACCCCTGACATAAAGTTG 3'
mIrx1_RT_fwd1 sense	5' ACCCAACTACAGCGCCTTCTT 3'
mIrx1_RT_rev1 antisense	5' TCATACTGAGAGCCCATCTGCG 3'
mItgb8_RT_fwd sense:	5' GCAGCCTGGGTATTTCAC 3'

mItgb8_RT_rev antisense:	5' GCACAGGAGACCACATTG 3'
mLhx2_RT_fwd sense:	5' GCAGCCAAAAGACAAAGCG 3'
mLhx2_RT_rev antisense:	5' GTAAAAGGTTGCGCCTGAAC 3'
mMadcam1_RT_fwd3 sense:	5' CCAATCTGTATGTTCTGGC 3'
mMadcam1_RT_rev3 antisense:	5' TCTCTGCCTCCTTAGTCTG 3'
mMmp9_RT_fwd sense:	5' GGACAGCCAGACACTAAAG 3'
mMmp9_RT_rev antisense:	5' CGGCAAGTCTTCAGAGTAG 3'
mNcam1_RT_fwd sense:	5' CCCACAGGAGTTAAGGAAG 3'
mNcam1_RT_rev antisense:	5' GGACAGGACTATGAACCG 3'
mNgfr_RT_fwd1 sense:	5' GCCTGGACAGTGTACGTTCTC 3'
mNgfr_RT_rev1 antisense:	5' CGGACATACTCTGCAGGCC 3'
mNrp1_RT_fwd sense:	5' TCCGAATCAAACCTGTATCCTG 3'
mNrp1_RT_rev antisense:	5' GATGCTGTAATCTGGAGTCTG 3'
mNrp2_RT_fwd sense:	5' TTCCTGACCTTGACCTG 3'
mNrp2_RT_rev antisense:	5' GGAGTTGGAGGGTGT 3'
mProkr2_RT_fwd sense:	5' CTCCGTCAACTACCTCGTAC 3'
mProkr2_RT_rev2 antisense:	5' GACCAAAGCGATCAGGAAGG 3'
mPthlh_RT_fwd sense:	5' GGAGTGTCTGGTATTCTG 3'
mPthlh_RT_rev antisense:	5' ACTTGCCTTGTACATGC 3'
mPtch1_RT_fwd sense:	5' GGTCTCGCTTACAAACTC 3'
mPtch1_RT_rev antisense:	5' CGGTCAAGGTAGATGTAGAAAG 3'
mPtch2_RT_fwd2 sense:	5' GCTTACTTCCAAGGTCTACTC 3'
mPtch2_RT_rev2 antisense:	5' AGTCTGAATCAACATCTGGG 3'
mRelb_RT_fwd2 sense:	5' GCTGTACTTGCTCTGTGAC 3'
mRelb_RT_rev2 antisense:	5' GGTGGCGTTTGAACAC 3'
mScube1_RT_fwd2 sense:	5' CCTTGCCCCAAACCAGAAAG 3'
mScube1_RT_rev2 antisense:	5' GACCATCTGCATGTAAGGC 3'
mSfrp1_RT_fwd sense:	5' CGGAAGCCTCTAACGCC 3'
mSfrp1_RT_rev antisense:	5' TCTTGTCAACCGTTTCCTTC 3'
mShh_RT_fwd sense:	5' GGCAGATATGAAGGGAAGATC 3'
mShh_RT_rev antisense:	5' CATTAACTTGTCTTGACCC 3'
mSox9_RT_fwd2 sense:	5' GCAAGACTCTGGCAAG 3'
mSox9_RT_rev2 antisense:	5' GCTGGTACTTGTAAATCGGG 3'
mSox21_RT_fwd sense:	5' TGGTGTGCTGTTGCACCTC 3'
mSox21_RT_rev antisense:	5' GGAGGGAGGAAGGATGAGAC 3'
mTnc_RT_fwd sense:	5' GAGGACTTCTATCGCAACTGG 3'
mTnc_RT_rev antisense:	5' CTTGGGCTGTGATTTGCTC 3'
mTnfaip3_RT_fwd2 sense:	5' GGAAACAGGACTTGCTACG3'
mTnfaip3_RT_rev2 antisense:	5' GATGTTGCTGAGGACAATATG3'
mTrps1_RT_fwd sense:	5' GCCATCCAAGACTTCCAG 3'
mTrps1_RT_rev antisense:	5' AGTTTCCGTCCAATGCC 3'
mTsku_RT_fwd sense:	5' GCTCCCCCTTGAGTGACATC 3'
mTsku_RT_rev antisense:	5' GGAAGCAGGCGATGGATAAG 3'
mTspan18_RT_fwd2 sense:	5' CTTACCAAGCACTACCAAGG 3'
mTspan18_RT_rev2 antisense:	5' TCAGTGTCCAGCGTCAG 3'
mWif1_RT_fwd sense:	5' CCACTCCATGAATTACCTG 3'
mWif1_RT_rev antisense:	5' AGGGACATTGACAGTTGG 3'

### Chromatin immunoprecipitation primers

Reference region:

mGapdh-ChIP-TSS-fwd sense: 5' GCCTGAGCTAGGACTGG 3'  
 mGapdh-ChIP-TSS-rev2 antisense: 5' AGGGCTGCAGTCGTATTTA 3'

NF-κB binding sites:

mLhx2-ChIP-+14550-fwd2 sense: 5' CATCCTGATTCCCTCTGGA 3'  
 mLhx2-ChIP-+14550-rev antisense: 5' GGGCTGACTTCTGCACCTT 3'  
 mSox9-ChIP-+2903-fwd2 sense: 5' CATTGCTGGAGGGAGAAAAG 3'

mSox9-ChIP-+2903-rev2 antisense:	5' GCCTAGAGGTGGATGGATGA 3'
mTrps1-ChIP--62449-fwd sense:	5' TGTTGCAGACCTAAGAAGGACA 3'
mTrps1-ChIP--62449-rev antisense:	5' CAACCTCACATGCCACACTT 3'
mMmp9-ChIP-+46fwd sense:	5' TCTTCCTCCCCAAGGAGT 3'
mMmp9-ChIP-+46rev antisense:	5' CCATCCCCACACTGTAGGTT 3'

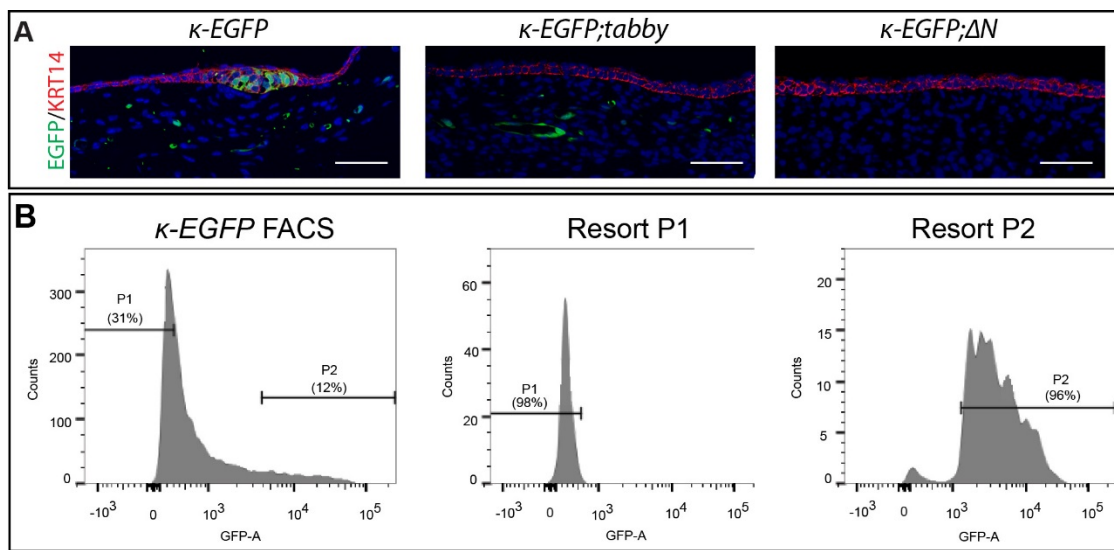


**Fig. S1. Isolation of primary placode keratinocytes using NF-κB-specific EGFP reporter mice ( $\kappa$ -EGFP).** (A) EGFP expression pattern in  $\kappa$ -EGFP,  $\kappa$ -EGFP;tabby and  $\kappa$ -EGFP; $\Delta$ N embryos at E14.5. (B) Enzymatically and mechanically separated epidermal keratinocytes from  $\kappa$ -EGFP embryos (n = 5) were sorted via FACS into an EGFP-positive (primary placode-specific, P2) and EGFP-negative (interfollicular keratinocytes, P1) cell population. Purity of both populations was determined over a resort, in which both populations showed a recovery rate of over 95%. Purified cell populations were used for microarray analysis, qRT-PCR and ChIP experiments.

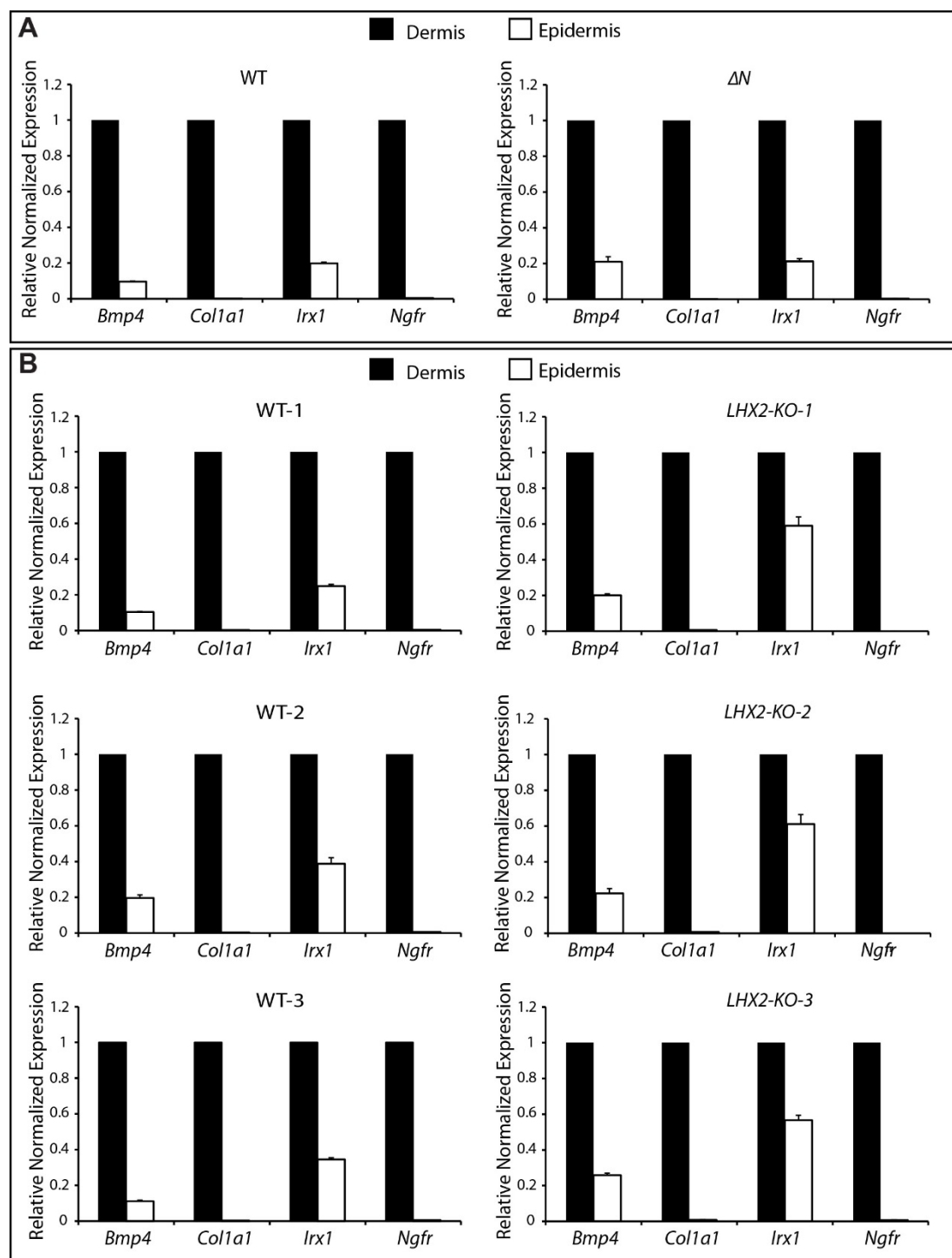


**Fig. S2. Dermal markers were absent in epidermal keratinocyte samples of  $\Delta N$ , *Lhx2*-KOs and of corresponding controls.** (A,B) Quantitative real-time PCR (qRT-PCR) analysis for *Bmp4*, *Col1a1*, *Irx1* and *Ngfr* expression using either RNA samples from epidermal keratinocytes of  $n = 3$   $\Delta N$  (A), *Lhx2*-KO (B) and corresponding control embryos at E14.5. Statistical analyses were performed using a two-tailed unpaired t-test. Data are presented as mean $\pm$ s.e.m.

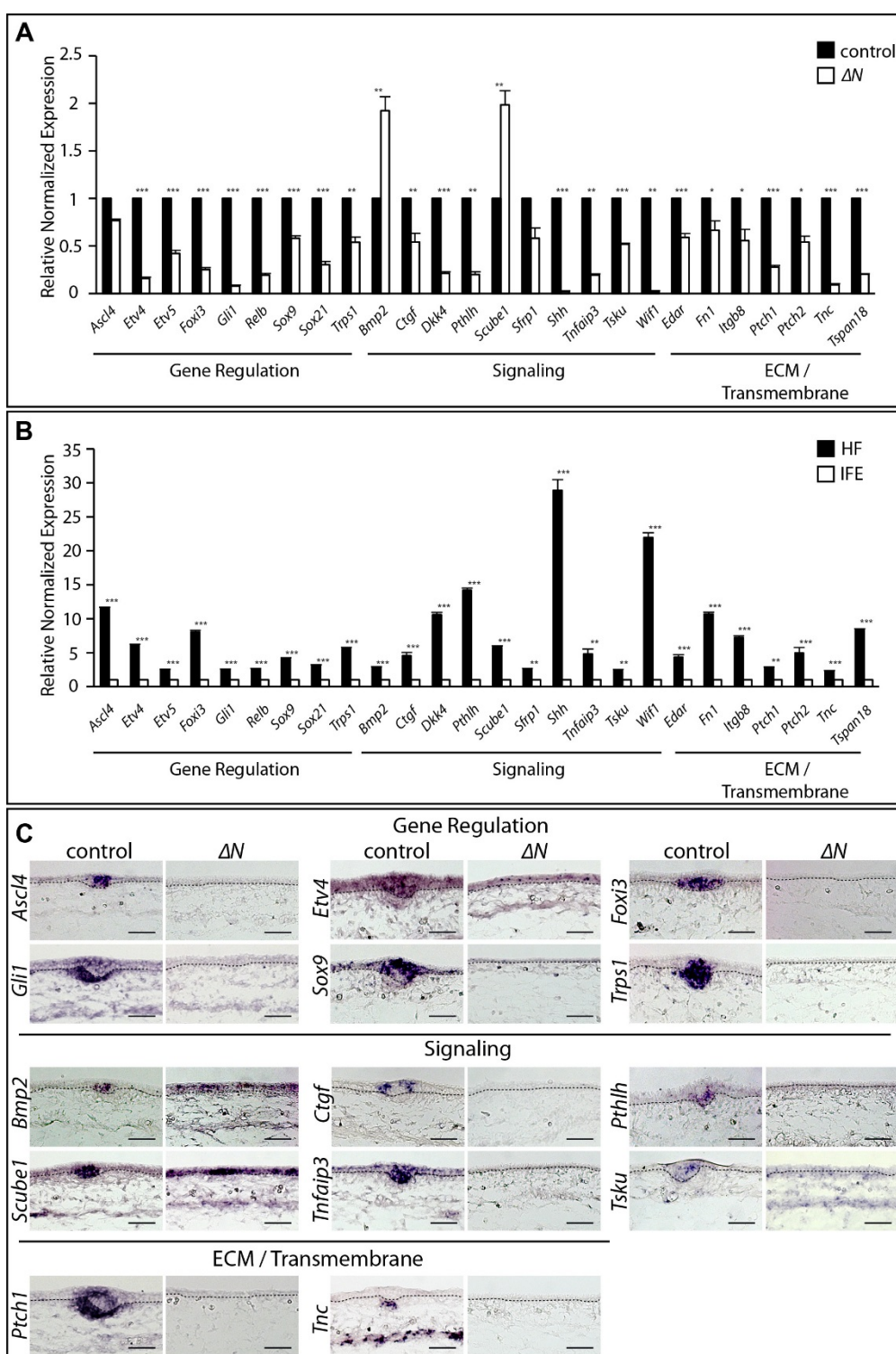


**Fig. S3. Verification of placode-specific expression and of NF- $\kappa$ B dependence of selected genes from microarray analysis.** **(A,B)** Quantitative real-time PCR (qRT-PCR) analysis using either RNA samples from epidermal keratinocytes of  $n = 3$  controls or  $\Delta N$  embryos **(A)**, or RNA samples isolated from EGFP- positive (placode) or EGFP-negative (IFE) sorted keratinocytes **(B)** at E14.5. Statistical analyses were performed using a two-tailed unpaired t-test. Data are presented as mean  $\pm$  s.e.m. \*  $P < 0.05$ ; \*\*  $P < 0.01$ ; \*\*\*  $P < 0.001$ . **(C)** In situ hybridization for mRNAs of NF- $\kappa$ B target genes using representative sagittal sections of  $n = 3$   $\Delta N$  and control embryos at E14.5. Dashed lines indicate boundary between epidermis and dermis. Scale bars: 50  $\mu$ m.

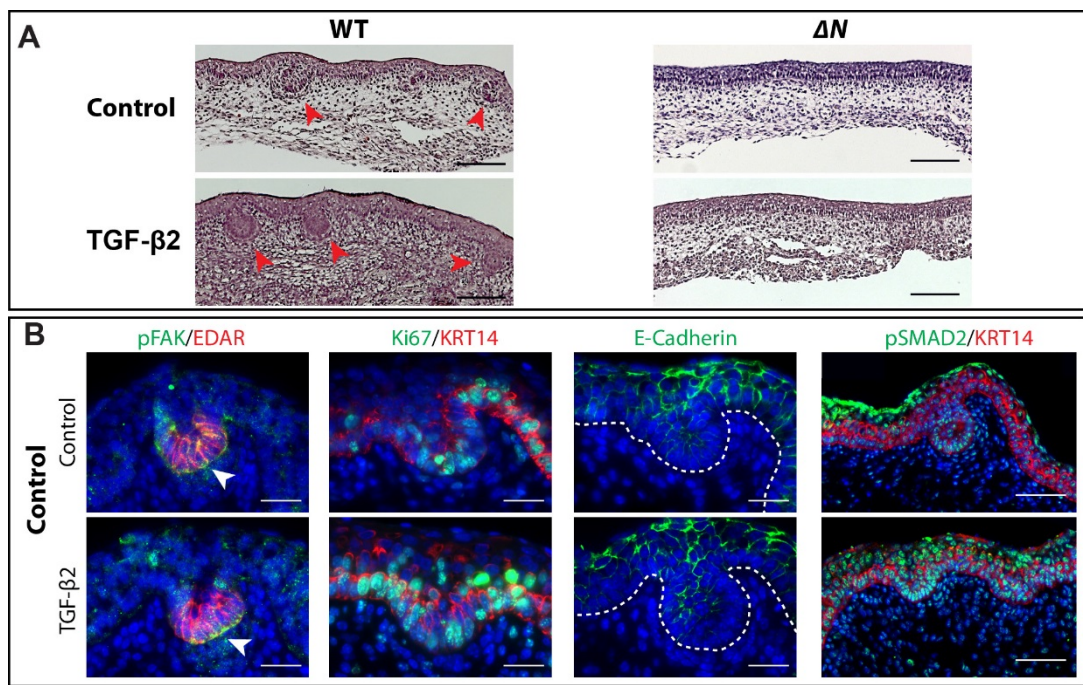


**Fig. S4. Treatment of embryonic control skin explants with recombinant TGF $\beta$ 2 slightly enhanced primary HF induction.** (A) Embryonic skin explants from  $n = 3$  E14.5 control and  $\Delta N$  embryos were either left untreated (Control) or treated with recombinant TGF $\beta$ 2 (100 ng/ml) for 24 hrs.  $n = 18$  samples of each experimental group were stained with H&E and follicles were quantified in numbers of hair follicle placodes/microscopic field in relation to the control group. Scale bars: 100 $\mu$ m. (B) Immunostaining on TGF- $\beta$ 2-stimulated embryonic control skin sections corresponding to E15.5 using antibodies against pFAK, Ki67 and E-Cadherin, as well as against EDAR and KRT14 to indicate placodes. Scale bars: 20  $\mu$ m / 50  $\mu$ m (pSMAD2). Arrowheads indicate pFAK expression in HF placodes; dashed lines delineate dermal-epidermal boundaries.

**Supplementary Table S1.** Representative lists of genes enriched in E14.5 primary hair follicle placodes (**upper list**) or in the interfollicular epidermis (IFE; **lower list**). Only mRNAs differentially regulated  $\geq 1.5x$  in **hair follicle placodes vs. IFE** are listed. Hair follicle placode keratinocytes correspond to EGFP-expressing and IFE keratinocytes to EGFP-non-expressing cells separated by FACS (see main text and Fig. S1).

**Genes enriched in primary hair follicle placodes at E14.5:**

Genes symbol	Description	Ref_Seq	Fold change
Frem1	Fras1 related extracellular matrix protein 1	NM_177863	6.72678
Dkk4	dickkopf homolog 4 (Xenopus laevis)	NM_145592	5.82304
Fn1	fibronectin 1	NM_010233	5.04024
Ascl4	achaete-scute complex homolog 4 (Drosophila)	NM_001163614	4.84369
Slc14a1	solute carrier family 14 (urea transporter), member 1	NM_001171010	4.59977
Trps1	trichorhinophalangeal syndrome I (human)	NM_032000	4.32476
Prokr2	prokineticin receptor 2	NM_144944	4.31001
Foxi3	forkhead box I3	NM_001101464	4.23003
Nrp2	neuropilin 2	NM_001077403	4.15898
Wif1	Wnt inhibitory factor 1	NM_011915	4.10489
Tspan18	tetraspanin 18	NM_183180	4.02829
Socs2	suppressor of cytokine signaling 2	NM_007706	3.96253
Ltb	lymphotoxin B	NM_008518	3.72502
Cd74	CD74 antigen	NM_001042605	3.448
Tgfb2	transforming growth factor, beta 2	NM_009367	3.40851
Necab1	N-terminal EF-hand calcium binding protein 1	NM_178617	3.33139
Fgf20	fibroblast growth factor 20	NM_030610	3.29271
Dusp6	dual specificity phosphatase 6	NM_026268	3.21706
Tmem100	transmembrane protein 100	NM_026433	3.17391
Edar	ectodysplasin-A receptor	NM_010100	3.15788
Rragd	Ras-related GTP binding D	NM_027491	3.11128
Itgb8	integrin beta 8	NM_177290	3.08216
Tll1	tolloid-like	NM_009390	3.07956
Mical2	microtubule associated monooxygenase, calponin and LIM domain containing 2	NM_177282	3.06069
Steap4	STEAP family member 4	NM_054098	3.0561
Adamts3	a disintegrin-like and metallopeptidase with thrombospondin motifs 3	NM_177872	2.97619
Has3	hyaluronan synthase 3	NM_008217	2.95032
Fgd5	FYVE, RhoGEF and PH domain containing 5	NM_172731	2.88688
Tnf	tumor necrosis factor	NM_013693	2.83063
Etv4	ets variant gene 4 (E1A enhancer binding protein, E1AF)	NM_008815	2.82086

Nkain3	Na+/K+ transporting ATPase interacting 3	NM_172987	2.77675
Shh	sonic hedgehog	NM_009170	2.76033
Prss35	protease, serine, 35	NM_178738	2.71064
Ifitm1	interferon induced transmembrane protein 1	NM_026820	2.7034
Lgr6	leucine-rich repeat-containing G protein-coupled receptor 6	NM_001033409	2.67464
Aff2	AF4/FMR2 family, member 2	NM_008032	2.67125
Clip3	CAP-GLY domain containing linker protein 3	NM_001081114	2.66474
C1s	complement component 1, s subcomponent	NM_144938	2.63794
Ncam1	neural cell adhesion molecule 1	NM_001081445	2.63623
Madcam1	mucosal vascular addressin cell adhesion molecule 1	NM_013591	2.63337
Cntnap1	contactin associated protein-like 1	NM_016782	2.62987
Rasgef1b	RasGEF domain family, member 1B	NM_145839	2.60963
Myb	myeloblastosis oncogene	NM_010848	2.59304
Moxid1	monooxygenase, DBH-like 1	NM_021509	2.59
Tnfaip3	tumor necrosis factor, alpha-induced protein 3	NM_009397	2.58453
Csgalnact1	chondroitin sulfate N-acetylgalactosaminyltransferase 1	NM_172753	2.58372
Mapk4	mitogen-activated protein kinase 4	NM_172632	2.5564
Stra6	stimulated by retinoic acid gene 6	NM_009291	2.55396
Krt17	keratin 17	NM_010663	2.55127
Kcnmb4	potassium large conductance calcium-activated channel, subfamily M beta member 4	NM_021452	2.53788
Mmp9	matrix metallopeptidase 9	NM_013599	2.53534
Srgap1	SLIT-ROBO Rho GTPase activating protein 1	NM_001081037	2.53366
Ctgf	connective tissue growth factor	NM_010217	2.50581
Stxbp6	syntaxin binding protein 6 (amisyn)	NM_144552	2.50082
Lass4	LAG1 homolog, ceramide synthase 4	NM_026058	2.47589
Scube1	signal peptide, CUB domain, EGF-like 1	NM_022723	2.46246
Cpe	carboxypeptidase E	NM_013494	2.4328
Pthlh	parathyroid hormone-like peptide	NM_008970	2.42713
Alox12e	arachidonate lipoxygenase, epidermal	NM_145684	2.42105
Ptch2	patched homolog 2	NM_008958	2.39458
Scd1	stearoyl-Coenzyme A desaturase 1	NM_009127	2.37643
Dchs1	dachsous 1 ( <i>Drosophila</i> )	NM_001162943	2.33643
Cyfip2	cytoplasmic FMR1 interacting protein 2	NM_133769	2.32122
Rhpn2	rhophilin, Rho GTPase binding protein 2	NM_027897	2.31369
Prnd	prion protein dublet	NM_023043	2.3072
Cxcr4	chemokine (C-X-C motif) receptor 4	NM_009911	2.30564
Cxcl9	chemokine (C-X-C motif) ligand 9	NM_008599	2.28395
Setbp1	SET binding protein 1	NM_053099	2.25846
Lgi2	leucine-rich repeat LGI family, member 2	NM_144945	2.2534

Sox9	SRY-box containing gene 9	NM_011448	2.24712
Fgfr1	fibroblast growth factor receptor 1	NM_010206	2.2423
Runx1	runt related transcription factor 1	NM_001111023	2.22868
Fndc1	fibronectin type III domain containing 1	NM_001081416	2.21535
Eif4e3	eukaryotic translation initiation factor 4E member 3	NM_025829	2.20993
Heg1	HEG homolog 1 (zebrafish)	NM_175256	2.1946
Lhx2	LIM homeobox protein 2	NM_010710	2.19298
Lrp4	low density lipoprotein receptor-related protein 4	NM_172668	2.18112
Ccdc85a	coiled-coil domain containing 85A	NM_181577	2.1585
Zdhhc2	zinc finger, DHHC domain containing 2	NM_178395	2.15626
Mill1	MHC I like leukocyte 1	NM_153749	2.14469
Micalcl	MICAL C-terminal like	AB359922	2.14146
Pstpip2	proline-serine-threonine phosphatase-interacting protein 2	NM_013831	2.08008
Il2rg	interleukin 2 receptor, gamma chain	NM_013563	2.06742
Bnc2	basonuclin 2	NM_172870	2.05488
Mybpc1	myosin binding protein C, slow-type	NM_175418	2.04995
Cabp1	calcium binding protein 1	NM_013879	2.0347
Kcnh3	potassium voltage-gated channel, subfamily H (eag-related) member 3	NM_010601	2.03291
Syt5	synaptotagmin V	NM_016908	2.02779
Fam13a	family with sequence similarity 13, member A	NM_153574	1.99645
Grik4	glutamate receptor, ionotropic, kainate 4	NM_175481	1.98605
1110012J17Rik	RIKEN cDNA 1110012J17 gene	NM_001114098	1.98034
Plk3	polo-like kinase 3 (Drosophila)	NM_013807	1.97215
Cxcl10	chemokine (C-X-C motif) ligand 10	NM_021274	1.96566
Ptch1	patched homolog 1	NM_008957	1.96207
Alcam	activated leukocyte cell adhesion molecule	NM_009655	1.93344
Tgfb1	transforming growth factor, beta 1	NM_011577	1.92935
Vldlr	very low density lipoprotein receptor	NM_013703	1.92326
Mpa2l	macrophage activation 2 like	NM_194336	1.92065
Wnt10b	wingless related MMTV integration site 10b	NM_011718	1.91905
Trib1	tribbles homolog 1 (Drosophila)	NM_144549	1.91708
Arhgef3	Rho guanine nucleotide exchange factor (GEF) 3	NM_027871	1.91348
H2-Ab1	histocompatibility 2, class II antigen A, beta 1	NM_207105	1.91304
C130021I20Rik	Riken cDNA C130021I20 gene	AK147796	1.90649
Mtmr10	myotubularin related protein 10	NM_172742	1.90315
Dab1	disabled homolog 1 (Drosophila)	NM_177259	1.89918
Wnt2b	wingless related MMTV integration site 2b	NM_009520	1.89907
Stx11	syntaxin 11	NM_029075	1.89836
Sv2b	synaptic vesicle glycoprotein 2 b	NM_001109753	1.89017

Nfkbia	nuclear factor of kappa light polypeptide gene enhancer in B-cells inhibitor alpha	NM_010907	1.88282
Rnf152	ring finger protein 152	NM_178779	1.87965
Fads2	fatty acid desaturase 2	NM_019699	1.87774
Gli1	GLI-Kruppel family member GLI1	NM_010296	1.87315
Pdzd2	PDZ domain containing 2	NM_001081064	1.86608
6330403K07Rik	RIKEN cDNA 6330403K07 gene	NM_134022	1.85268
Nr3c2	nuclear receptor subfamily 3, groupC, member2	NM_001083906	1.83938
Krt18	keratin 18	NM_010664	1.83723
Etv5	ets variant gene 5	NM_023794	1.8353
Kcnh2	potassium voltage-gated channel, subfamily H (eag-related) member 2	NM_013569	1.83401
Ptgir	prostaglandin I receptor (IP)	NM_008967	1.83208
Sh3rf3	SH3 domain containing ring finger 3	NM_172788	1.8301
Ptk2b	PTK2 protein tyrosine kinase 2 beta	NM_001162365	1.82897
Mtap2	microtubule-associated protein 2	NM_001039934	1.82823
Mtmr7	myotubularin related protein 7	NM_001040699	1.82822
Robo2	roundabout homolog 2 (Drosophila)	NM_175549	1.82721
Kalrn	kalirin, RhoGEF kinase	NM_177357	1.8251
Bcl3	B-cell leukemia/lymphoma 3	NM_033601	1.82083
Tarm1	T cell-interacting, activating receptor on myeloid cells 1	NM_177363	1.80831
Rerg	RAS-like, estrogen-regulated, growth-inhibitor	NM_181988	1.80721
Pgf	placental growth factor	NM_008827	1.80406
Stap1	signal transducing adaptor family member 1	NM_019992	1.80181
Adamts15	a disintegrin-like and metallopeptidase with thrombospondin motifs 15	NM_001024139	1.78899
Nnat	neuronatin	NM_010923	1.78484
3110082D06Rik	RIKEN cDNA 3110082D06 gene	NM_028474	1.77842
Peli2	pellino 2	NM_033602	1.77669
Unc5b	unc-5 homolog B (C. elegans)	NM_029770	1.77391
Tspan5	tetraspanin 5	NM_019571	1.77279
Galnt6	UDP-N-acetyl-alpha-D-galactosamine: polypeptide N-acetylgalactosaminyltransferase 6	NM_001161767	1.7722
Pion	pigeon homolog (Drosophila)	NM_175437	1.76624
Kcnip1	Kv channel-interacting protein 1	NM_027398	1.76196
Drp2	dystrophin related protein 2	NM_010078	1.76107
Neto1	neuropilin (NRP) and tollloid (TLL)-like 1	NM_144946	1.75975
Serinc2	serine incorporator 2	NM_172702	1.75794
Bach2	BTB and CNC homology 2	NM_001109661	1.75674
Ptges	prostaglandin E synthase	NM_022415	1.75584
Tapbp	TAP binding protein	NM_001025313	1.75121
Plcb2	phospholipase C, beta 2	NM_177568	1.74533

Meis1	Meis homeobox 1	NM_010789	1.73948
Ajap1	adherens junction associated protein 1	NM_001099299	1.73929
Sh3gl3	SH3-domain GRB2-like 3	NM_017400	1.73684
Sema3d	sema domain, immunoglobulin domain (Ig), short basic domain secreted (semaphorin) 3D	NM_028882	1.73535
Sox2	SRY-box containing gene 2	NM_011443	1.7348
Hhip	Hedgehog-interacting protein	NM_020259	1.73156
Hoxc6	homeobox C6	NM_010465	1.72724
Tsku	tsukushin	NM_001168541	1.72657
Rtn1	reticulon 1	NM_153457	1.72548
Smox	spermine oxidase	NM_001177833	1.72453
Pxdn	peroxidasin homolog (Drosophila)	NM_181395	1.71855
AY512949	cDNA sequence AY512949	AY512949	1.71621
Rcn3	reticulocalbin 3, EF-hand calcium binding domain	NM_026555	1.71433
Rnf32	ring finger protein 32	NM_021470	1.711
Il23a	interleukin 23, alpha subunit p19	NM_031252	1.70695
Cpne5	copine V	NM_153166	1.70401
Slit3	slit homolog 3 (Drosophila)	NM_011412	1.70263
Susd4	sushi domain containing 4	NM_144796	1.70162
Atp1b1	ATPase, Na+/K+ transporting, beta 1 polypeptide	NM_009721	1.69741
Sox21	SRY-box containing gene 21	NM_177753	1.69563
Bmp2	bone morphogenetic protein 2	NM_007553	1.69554
2010300C02Rik	RIKEN cDNA 2010300C02 gene	NM_028096	1.68928
Sema4c	sema domain, immunoglobulin domain (Ig), transmembrane domain (TM) and short cytoplasmic domain, (Semaphorin) 4C	NM_001126047	1.68679
Cacna1h	calcium channel, voltage-dependent, T type, alpha 1H subunit	NM_021415	1.68588
1110028C15Rik	RIKEN cDNA 1110028C15 gene	NM_001122738	1.68216
D19Ert652e	DNA segment, Chr 19, ERATO Doi 652, expressed	BC107403	1.68043
Igfbp4	insulin-like growth factor binding protein 4	NM_010517	1.68001
Slco3a1	solute carrier organic anion transporter family, member 3A1	NM_023908	1.67316
Cntn2	contactin 2	NM_177129	1.66761
Gm5077	predicted gene 5077	NM_173864	1.66026
Runx2	runt related transcription factor 2	NM_001146038	1.65805
Clec2d	C-type lectin domain family 2, member d	NM_053109	1.65631
Ptgs2	prostaglandin-endoperoxide synthase 2	NM_011198	1.65597
Ehf	ets homologous factor	NM_007914	1.65559
Hr	hairless	NM_021877	1.65486
Arl6	ADP-ribosylation factor-like 6	NM_019665	1.6485

Nup210	nucleoporin 210	NM_018815	1.6388
Rnf122	ring finger protein 122	NM_175136	1.63805
Galnt14	UDP-N-acetyl-alpha-D-galactosamine: polypeptide N-acetylgalactosaminyltransferase 14	NM_027864	1.63479
Bcar3	breast cancer anti-estrogen resistance 3	NM_013867	1.63365
Doc2b	double C2, beta	NM_007873	1.63109
Gpc2	glypican 2 (cerebroglycan)	NM_172412	1.63104
Mfap2	microfibrillar-associated protein 2	NM_008546	1.6301
Parp8	poly (ADP-ribose) polymerase family, member 8	NM_001081009	1.62741
Csf1	colony stimulating factor 1 (macrophage)	NM_007778	1.62535
Hpcal	hippocalcin	NM_010471	1.62412
Robo1	roundabout homolog 1 (Drosophila)	NM_019413	1.62296
Gata6	GATA binding protein 6	NM_010258	1.62065
Slc2a4	solute carrier family 2 (facilitated glucose transporter) member 4	NM_009204	1.61892
Tnip1	TNFAIP3 interacting protein 1	NM_021327	1.61539
Snai3	snail homolog 3 (Drosophila)	NM_013914	1.61109
Adamts17	a disintegrin-like and metallopeptidase with thrombospondin motifs 17	NM_001033877	1.61011
Slc39a2	solute carrier family 39 (zinc transporter), member 2	NM_001039676	1.60699
Ntsr1	neurotensin receptor 1	NM_018766	1.60654
Ston2	stonin 2	NM_175367	1.60549
Chst1	carbohydrate (keratan sulfate Gal-6) sulfotransferase 1	NM_023850	1.60363
Igfbp7	insulin-like growth factor binding protein 7	NM_001159518	1.60225
Pdlim4	PDZ and LIM domain 4	NM_019417	1.6007
Flrt1	fibronectin leucine rich transmembrane protein 1	NM_201411	1.6
Ankrd45	ankyrin repeat domain 45	NM_028664	1.59378
Scn4b	sodium channel, type IV, beta	NM_001013390	1.59078
Ifitm3	interferon induced transmembrane protein 3	NM_025378	1.5882
Vwa2	von Willebrand factor A domain containing 2	NM_172840	1.58769
Zfp703	zinc finger protein 703	NM_001101502	1.58643
Aplp1	amyloid beta (A4) precursor-like protein 1	NM_007467	1.58109
Pcdh20	protocadherin 20	NM_178685	1.5777
Efha2	EF-hand domain family, member A2	NM_030110	1.57743
Ctxn1	cortexin 1	NM_183315	1.57693
Pcdhb17	protocadherin beta 17	NM_053142	1.5748
Sox4	SRY-box containing gene 4	NM_009238	1.57435
Birc3	baculoviral IAP repeat-containing 3	NM_007464	1.56615
Pcdhb16	protocadherin beta 16	NM_053141	1.566
Gria3	glutamate receptor, ionotropic, AMPA3 (alpha 3)	NM_016886	1.56142

Itga8	integrin alpha 8	NM_001001309	1.55968
Cobll1	Cobl-like 1	NM_177025	1.55902
Mpped1	metallophosphoesterase domain containing 1	NM_172610	1.55823
Tnc	tenascin C	NM_011607	1.55711
Fam134b	family with sequence similarity 134, member B	NM_001034851	1.5547
Bdnf	brain derived neurotrophic factor	NM_001048139	1.55203
Pfn2	profilin 2	NM_019410	1.55202
Ednra	endothelin receptor type A	NM_010332	1.55142
Ltbp1	latent transforming growth factor beta binding protein 1	NM_019919	1.54781
Orai2	ORAI calcium release-activated calcium modulator 2	NM_178751	1.54545
Prkar1b	protein kinase, cAMP dependent regulatory, type I beta	NM_008923	1.54434
Oasl2	2'-5' oligoadenylate synthetase-like 2	NM_011854	1.5437
Pck2	phosphoenolpyruvate carboxykinase 2 (mitochondrial)	NM_028994	1.543
Kcnj13	potassium inwardly-rectifying channel, subfamily J, member 13	NM_001110227	1.54167
Lzts1	leucine zipper, putative tumor suppressor 1	NM_199364	1.54108
Grasp	GRP1 (general receptor for phosphoinositides 1)-associated scaffold protein	NM_019518	1.54028
Abhd12b	abhydrolase domain containing 12B	ENSMUST00000095662	1.53875
Olfr332	olfactory receptor 332	NM_001011770	1.53477
Olfr354	olfactory receptor 354	NM_146939	1.53475
Slc8a2	solute carrier family 8 (sodium/calcium exchanger), member 2	NM_148946	1.53388
H2-M2	histocompatibility 2, M region locus 2	NM_008204	1.53362
Gpc4	glypican 4	NM_008150	1.52993
Sema6a	sema domain, transmembrane domain (TM), and cytoplasmic domain (semaphorin) 6A	NM_018744	1.52824
Sfrp1	secreted frizzled-related protein 1	NM_013834	1.52721
Tcerg1l	transcription elongation regulator 1-like	NM_183289	1.52632
Prdm1	PR domain containing 1, with ZNF domain	NM_007548	1.52515
Pak1	p21 protein (Cdc42/Rac)-activated kinase 1	NM_011035	1.52389
1190007F08Rik	RIKEN cDNA 1190007F08 gene	NM_001163721	1.5194
Soat1	sterol O-acyltransferase 1	NM_009230	1.51793
Tgfb3	transforming growth factor, beta 3	NM_009368	1.51763
Rnf180	ring finger protein 180	NM_027934	1.51676
Capsl	calcybosine-like	NM_029341	1.51458
Ppp1r3c	protein phosphatase 1, regulatory (inhibitor) subunit 3C	NM_016854	1.5111
Argef4	Rho guanine nucleotide exchange factor (GEF) 4	NM_183019	1.51105
Spo11	sporulation protein, meiosis-specific, SPO11	NM_012046	1.51063

	homolog		
Chst11	carbohydrate sulfotransferase 11	NM_021439	1.51022
Mylip	myosin regulatory light chain interacting protein	NM_153789	1.50443
Lrrc56	leucine rich repeat containing 56	NM_001172064	1.50368
Serpincb6b	serine (or cysteine) peptidase inhibitor, clade B, member 6	NM_011454	1.5019
Myo1e	myosin IE	NM_181072	1.50175
Cav2	caveolin 2	NM_016900	1.50146
4831426l19Rik	RIKEN cDNA 4831426l19 gene	NM_001042699	1.50112
Naaladl2	N-acetylated alpha-linked acidic dipeptidase-like 2	XM_910834	1.50034

### **Genes enriched in the interfollicular epidermis (IFE) at E14.5:**

Genes symbol	Description	Ref_Seq	Fold change
Dct	dopachrome tautomerase	NM_010024	-13.3986
Fabp7	fatty acid binding protein 7, brain	NM_021272	-11.1386
Kit	kit oncogene	NM_001122733	-8.89564
Ednrb	endothelin receptor type B	NM_007904	-8.03849
Mcoln3	mucolipin 3	NM_134160	-7.67076
Hba-a1	hemoglobin alpha, adult chain 1	NM_008218	-7.59276
Hba-a2	hemoglobin alpha, adult chain 2	NM_001083955	-7.07394
Tyr	tyrosinase	NM_011661	-7.05902
Si	silver	NM_021882	-6.53347
Slc45a2	solute carrier family 45, member 2	NM_053077	-6.52809
Mitf	microphthalmia-associated transcription factor	NM_001113198	-6.29898
Hbb-b1	hemoglobin, beta adult major chain	NM_008220	-6.28766
Slc24a5	solute carrier family 24, member 5	NM_175034	-6.27844
Gpnmb	glycoprotein (transmembrane) nmb	NM_053110	-6.06478
Itga4	integrin alpha 4	NM_010576	-6.03604
Slc7a8	solute carrier family 7 (cationic amino acid transporter, light chain, L system) member 8	NM_016972	-5.91936
Gjc3	gap junction protein, gamma 3	NM_080450	-5.91203
Gabbrb2	gamma-aminobutyric acid (GABA) A receptor, subunit beta 2	NM_008070	-5.76314
Cubn	cubilin (intrinsic factor-cobalamin receptor)	NM_001081084	-5.7264
Bace2	beta-site APP-cleaving enzyme 2	NM_019517	-5.30143
Pax3	paired box gene 3	NM_008781	-5.15059
Zeb2	zinc finger E-box binding homeobox 2	NM_015753	-5.10228

Slc7a11	solute carrier family 7 (cationic amino acid transporter, light chain, L system) member 11	NM_011990	-5.00851
Gucy1b3	guanylate cyclase 1, soluble, beta 3	NM_017469	-4.68383
Shc4	SHC (Src homology 2 domain containing) family, member 4	NM_199022	-4.51824
Dsc1	desmocollin 1	NM_013504	-4.29284
Cd97	CD97 antigen	NM_011925	-4.08062
Pde8a	phosphodiesterase 8A	NM_008803	-4.01469
Cpa3	carboxypeptidase A3, mast cell	NM_007753	-3.96657
Ptpkj	protein tyrosine phosphatase, receptor type, J	NM_008982	-3.86641
Eya1	eyes absent 1 homolog (Drosophila)	NM_010164	-3.82696
Them5	thioesterase superfamily member 5	NM_025416	-3.79337
Tm4sf1	transmembrane 4 superfamily member 1	NM_008536	-3.7218
Serpinb12	serine (or cysteine) peptidase inhibitor, clade B (ovalbumin) member 12	NM_027971	-3.55006
Abca12	ATP-binding cassette, sub-family A (ABC1), member 12	NM_175210	-3.54327
1700086L19Rik	RIKEN cDNA 1700086L19 gene	NR_030733	-3.53514
Ttyh2	tweety homolog 2 (Drosophila)	NM_053273	-3.48151
Sox10	SRY-box containing gene 10	NM_011437	-3.40337
Bhlhe41	basic helix-loop-helix family, member e41	NM_024469	-3.36134
Pmp22	peripheral myelin protein 22	NM_008885	-3.35803
Cdh19	cadherin 19, type 2	NM_001081386	-3.33919
Aadac12	arylacetamide deacetylase-like 2	NM_001128091	-3.31869
Megf10	multiple EGF-like-domains 10	NM_001001979	-3.285
4833423E24Rik	RIKEN cDNA 4833423E24 gene	NM_001081664	-3.28403
Ddah1	dimethylarginine dimethylaminohydrolase 1	NM_026993	-3.27234
Serpinb3a	serine (or cysteine) peptidase inhibitor, clade B (ovalbumin) member 3	NM_009126	-3.19283
Elov14	elongation of very long chain fatty acids (FEN1/Elo2, SUR4/Elo3, Yeast)-Like 4	NM_148941	-3.17368
Iqgap2	IQ motif containing GTPase activating protein 2	NM_027711	-3.1546
Krt77	keratin 77	NM_001003667	-3.07428
Ace2	angiotensin I converting enzyme (peptidyl-dipeptidase A) 2	NM_027286	-3.06103
Serpinb3c	serine (or cysteine) peptidase inhibitor, clade B, member 3	NM_201363	-2.99416
Mlana	melan-A	NM_029993	-2.96325
Npy	neuropeptide Y	NM_023456	-2.94426
Aff3	AF4/FMR2 family, member 3	NM_010678	-2.91408
Dpbht2	DNA binding protein with his-thr domain	NM_198866	-2.88289
Casp14	caspase 14	NM_009809	-2.86772
Plp1	Nproteolipid protein (myelin) 1	NM_011123	-2.85823
Rdh12	retinol dehydrogenase 12	NM_030017	-2.85649

Cdh2	cadherin 2	NM_007664	-2.84678
Foxd3	forkhead box D3	NM_010425	-2.80057
Ptgds	prostaglandin D2 synthase (brain)	NM_008963	-2.7837
Fap	fibroblast activation protein	NM_007986	-2.78074
Krtdap	keratinocyte differentiation associated protein	NM_001033131	-2.73273
Sdr16c6	short chain dehydrogenase/reductase family 16C, member 6	NM_001080710	-2.693
Car8	carbonic anhydrase 8	NM_007592	-2.68262
Ctnnbp2	cortactin binding protein 2	NM_080285	-2.6631
Bpil2	bactericidal/permeability-increasing protein-like 2	NM_177772	-2.65552
Dmkn	dermokine	NM_001166173	-2.65336
Gabbrb3	gamma-aminobutyric acid (GABA) A receptor, subunit beta 3	NM_008071	-2.62234
Muc15	mucin 15	NM_172979	-2.61603
Glccl1	glucocorticoid induced transcript 1	NM_133236	-2.59503
Dock5	dedicator of cytokinesis 5	NM_177780	-2.56376
Tgm3	transglutaminase 3, E polypeptide	NM_009374	-2.56111
Vim	vimentin	NM_011701	-2.55643
Ets1	E26 avian leukemia oncogene 1, 5' domain	NM_011808	-2.54204
Lix1l	Lix1-like	NM_001163170	-2.53879
Smpdl3a	sphingomyelin phosphodiesterase, acid-like 3A	NM_020561	-2.53731
Glrb	glycine receptor, beta subunit	NM_010298	-2.53534
Pnpla1	patatin-like phospholipase domain containing 1	NM_001034885	-2.52928
Rhoj	ras homolog gene family, member J	NM_023275	-2.52197
Lmo2	LIM domain only 2	NM_008505	-2.51665
Gpr124	G protein-coupled receptor 124	NM_054044	-2.51493
Eng	endoglin	NM_001146350	-2.51234
Cyp4f39	cytochrome P450, family 4, subfamily f, polypeptide 39	NM_177307	-2.47551
Hspb1	heat shock protein 1	NM_013560	-2.46524
Dsg1a	desmoglein 1 alpha	NM_010079	-2.4552
Gabra1	gamma-aminobutyric acid (GABA) A receptor, subunit alpha 1	NM_010250	-2.44598
Rassf2	Ras association (RalGDS/AF-6) domain family member 2	NM_175445	-2.40868
Fndc3c1	fibronectin type III domain containing 3C1	NM_001007580	-2.39585
Mef2c	myocyte enhancer factor 2C	NM_001170537	-2.39039
Pla2g2f	phospholipase A2, group IIF	NM_012045	-2.37833
Krt1	keratin 1	NM_008473	-2.37567
Cyp2j6	cytochrome P450, family 2, subfamily j, polypeptide 6	NM_010008	-2.36934
Gpm6a	glycoprotein m6a	NM_153581	-2.36615

Cd44	CD44 antigen	NM_009851	-2.36345
2610528A11Rik	RIKEN cDNA 2610528A11 gene	BC049685	-2.35047
Serpinb3b	serine (or cysteine) peptidase inhibitor, clade B (ovalbumin) member 3	NM_198680	-2.34213
Ly6g6c	lymphocyte antigen 6 complex, locus G6C	NM_023463	-2.33239
Syt4	synaptotagmin IV	NM_009308	-2.32023
Aox4	aldehyde oxidase 4	NM_023631	-2.29538
Dusp4	dual specificity phosphatase 4	NM_176933	-2.28567
Cyp2w1	cytochrome P450, family 2, subfamily w, polypeptide 1	NM_001160265	-2.28215
Tspan10	tetraspanin 10	NM_145363	-2.2754
Gpr111	G protein-coupled receptor 111	NM_001033493	-2.24943
Lgals9	lectin, galactose binding, soluble 9	NM_010708	-2.24754
Krt10	keratin 10	NM_010660	-2.24585
Acsl1	acyl-CoA synthetase long-chain family member 1	NM_007981	-2.24443
C130079G13Rik	RIKEN cDNA C130079G13 gene	NM_177661	-2.2349
Sdr16c5	short chain dehydrogenase/reductase family 16C, member 5	NM_181989	-2.23471
Dgat2	diacylglycerol O-acyltransferase 2	NM_026384	-2.22619
Tspan7	tetraspanin 7	NM_019634	-2.22509
Ceacam1	carcinoembryonic antigen-related cell adhesion molecule 1	NM_001039185	-2.21668
Plxna4	plexin A4	NM_175750	-2.21437
Mgst1	microsomal glutathione S-transferase 1	NM_019946	-2.21317
Tmem45a	transmembrane protein 45a	NM_019631	-2.21307
Ephx3	epoxide hydrolase 3	NM_001033163	-2.20599
Igf1	insulin-like growth factor 1	NM_010512	-2.19222
Nkd2	naked cuticle 2 homolog (Drosophila)	NM_028186	-2.18762
Gpr155	G protein-coupled receptor 155	NM_001080707	-2.17668
Mgl1	monoglyceride lipase	NM_001166251	-2.1652
Loxl3	lysyl oxidase-like 3	NM_013586	-2.16268
Lgals3	lectin, galactose binding, soluble 3	NM_001145953	-2.15513
Dhrs7	dehydrogenase/reductase (SDR family) member 7	NM_025522	-2.14505
Defb1	defensin beta 1	NM_007843	-2.13563
Igfsf11	immunoglobulin superfamily, member 11	NM_170599	-2.13439
Apod	apolipoprotein D	NM_007470	-2.12285
Ano7	anoctamin 7	NM_207031	-2.11815
Msn	moesin	NM_010833	-2.11068
Gsta1	glutathione S-transferase, alpha 1 (Ya)	NM_008181	-2.10006
Alx1	ALX homeobox 1	NM_172553	-2.07513
Qpct	glutaminyl-peptide cyclotransferase (glutaminyl cyclase)	NM_027455	-2.05609

Pcsk2	proprotein convertase subtilisin/kexin type 2	NM_008792	-2.04744
Lox	lysyl oxidase	NM_010728	-2.04368
Tgm1	transglutaminase 1, K polypeptide	NM_001161715	-2.01038
Rxrg	retinoid X receptor gamma	NM_009107	-2.00772
Itga9	integrin alpha 9	NM_133721	-2.00334
Fam174b	family with sequence similarity 174, member B	NM_001162532	-1.99666
Trf	transferrin	NM_133977	-1.99192
St8sia6	ST8 alpha-N-acetyl-neuraminide alpha-2,8-sialyltransferase 6	NM_145838	-1.99135
Tmem26	transmembrane protein 26	NM_177794	-1.99127
Dpysl3	dihydropyrimidinase-like 3	NM_009468	-1.98497
Myo7a	myosin VIIA	NM_008663	-1.98315
Chsy3	chondroitin sulfate synthase 3	NM_001081328	-1.98098
Dsg1b	desmoglein 1 beta	NM_181682	-1.97908
Hsd17b11	hydroxysteroid (17-beta) dehydrogenase 11	NM_053262	-1.97763
Npbwr1	neuropeptides B/W receptor 1	NM_010342	-1.9776
Clvs1	clavesin 1	NM_028940	-1.97621
Gca	grancalcin	NM_145523	-1.97335
Mocos	molybdenum cofactor sulfurase	NM_026779	-1.9684
Gm10639	predicted gene 10639	NM_001122660	-1.96733
Mme	membrane metallo endopeptidase	NM_008604	-1.95696
Fmn1	formin 1	NM_010230	-1.95256
Gsta2	glutathione S-transferase, alpha 2 (Yc2)	NM_008182	-1.93678
Nipal1	NIPA-like domain containing 1	NM_001081205	-1.93147
Rab25	RAB25, member RAS oncogene family	NM_016899	-1.93048
Gldc	glycine decarboxylase	NM_138595	-1.92331
F3	coagulation factor III	NM_010171	-1.92279
Pde3a	phosphodiesterase 3A, cGMP inhibited	NM_018779	-1.92154
Slc6a15	solute carrier family 6 (neurotransmitter transporter), member 15	NM_175328	-1.92055
Scel	sciellin	NM_022886	-1.91843
Atg4a	autophagy-related 4A (yeast)	NM_174875	-1.91751
Nipal4	NIPA-like domain containing 4	NM_172524	-1.89996
St3gal5	ST3 beta-galactoside alpha-2,3-sialyltransferase 5	NM_011375	-1.89425
Tprg	transformation related protein 63 regulated	NM_175165	-1.89031
Plxnc1	plexin C1	NM_018797	-1.88757
Pcsk6	proprotein convertase subtilisin/kexin type 6	NM_011048	-1.88695
Vat1l	vesicle amine transport protein 1 homolog-like	NM_173016	-1.88139
Phyhipl	phytanoyl-CoA hydroxylase interacting protein-like	NM_178621	-1.88025
Hexa	hexosaminidase A	NM_010421	-1.87951
Fam13c	family with sequence similarity 13, member C	NM_024244	-1.87934

Acadl	acyl-Coenzyme A dehydrogenase, long-chain	NM_007381	-1.87602
Parvb	parvin, beta	NM_133167	-1.86923
Gabrp	gamma-aminobutyric acid (GABA) A receptor, pi	NM_146017	-1.86752
Smtnl2	smoothelin-like 2	NM_177776	-1.86721
Cpa6	carboxypeptidase A6	NM_177834	-1.8646
Lipm	lipase, family member M	NM_023903	-1.86238
Dpp4	dipeptidylpeptidase 4	NM_010074	-1.86079
Anxa1	annexin A1	NM_010730	-1.86048
Afaf1l2	actin filament associated protein 1-like 2	NM_146102	-1.85728
Heyl	hairy/enhancer-of-split related with YRPW motif-like	NM_013905	-1.85722
Zfp185	zinc finger protein 185	NM_009549	-1.85238
Atg4a	autophagy-related 4A (yeast)	NM_174875	-1.85005
Ch25h	cholesterol 25-hydroxylase	NM_009890	-1.85
4931406C07Rik	RIKEN cDNA 4931406C07 gene	NM_133732	-1.848
Slc2a3	solute carrier family 2 (facilitated glucose transporter) member 3	NM_011401	-1.84559
Col12a1	collagen, type XII, alpha 1	NM_007730	-1.8431
Sgip1	SH3-domain GRB2-like (endophilin) interacting protein 1	NM_144906	-1.84309
Adam12	a disintegrin and metallopeptidase domain 12 (meltrin alpha)	NM_007400	-1.84139
Gulp1	GULP, engulfment adaptor PTB domain containing 1	NM_028450	-1.84102
Fam57a	family with sequence similarity 57, member A	NM_027773	-1.8401
Ccr4	chemokine (C-C motif) receptor 4	NM_009916	-1.83905
Plagl1	pleiomorphic adenoma gene-like 1	NM_009538	-1.83139
Tmem154	transmembrane protein 154	NM_177260	-1.83136
St3gal1	ST3 beta-galactoside alpha-2,3-sialyltransferase 1	NM_009177	-1.82318
Crmp1	collapsin response mediator protein 1	NM_007765	-1.81883
Il22ra1	interleukin 22 receptor, alpha 1	NM_178257	-1.81498
Cftr	cystic fibrosis transmembrane conductance regulator homolog	NM_021050	-1.81473
Ctsc	cathepsin C	NM_009982	-1.81255
Tnik	TRAF2 and NCK interacting kinase	NM_026910	-1.8114
Sbsn	suprabasin	NM_172205	-1.81113
Chl1	cell adhesion molecule with homology to L1CAM	NM_007697	-1.80492
Uap1l1	UDP-N-acetylglucosamine pyrophosphorylase 1-like 1	NM_001033293	-1.79965
Pcbd1	pterin 4 alpha carbinolamine dehydratase/dimerization cofactor of Hepatocyte Nuclear Factor 1 Alpha	NM_025273	-1.79887

Pde3b	phosphodiesterase 3B, cGMP-inhibited	NM_011055	-1.79598
Arhgap6	Rho GTPase activating protein 6	NM_009707	-1.79047
Ceacam19	carcinoembryonic antigen-related cell adhesion molecule 19	NM_177036	-1.78945
Adamts1	a disintegrin-like and metallopeptidase reproblysin type with Thrombospondin Type 1 Motif, 1	NM_009621	-1.78818
Rab31	RAB31, member RAS oncogene family	NM_133685	-1.78794
Nppb	natriuretic peptide precursor type B	NM_008726	-1.78734
Cdh9	cadherin 9	NM_009869	-1.78631
Adssl1	adenylosuccinate synthetase like 1	NM_007421	-1.78417
Edn1	endothelin 1	NM_010104	-1.78375
Lypd3	Ly6/Plaur domain containing 3	NM_133743	-1.78152
Capns2	calpain, small subunit 2	NM_027112	-1.78084
2310007B03Rik	RIKEN cDNA 2310007B03 gene	NM_172411	-1.77783
Anxa8	annexin A8	NM_013473	-1.77481
Ppp1r16b	protein phosphatase 1, regulatory (inhibitor) subunit 16	NM_153089	-1.76265
Rin3	Ras and Rab interactor 3	NM_177620	-1.7594
Aim1	absent in melanoma 1	NM_172393	-1.75903
Gm5226	predicted pseudogene 5226	XM_914955	-1.75671
Ogn	osteoglycin	NM_008760	-1.75611
Manba	mannosidase, beta A, lysosomal	NM_027288	-1.75238
2210023G05Rik	RIKEN cDNA 2210023G05 gene	NM_197999	-1.7485
Slc26a7	solute carrier family 26, member 7	NM_145947	-1.7447
Cd200	CD200 antigen	NM_010818	-1.744
Rab3d	RAB3D, member RAS oncogene family	NM_031874	-1.7392
Leprel1	leprecan-like 1	NM_173379	-1.73852
AW551984	expressed sequence AW551984	NM_178737	-1.7381
C2	complement component 2 (within H-2S)	NM_013484	-1.73393
Scnn1a	sodium channel, nonvoltage-gated 1 alpha	NM_011324	-1.73157
Il15	interleukin 15	NM_008357	-1.73129
Sirpa	signal-regulatory protein alpha	NM_007547	-1.72769
Dlx5	distal-less homeobox 5	NM_010056	-1.727
Hist1h2bc	histone cluster 1, H2bc	NM_023422	-1.72637
Nkain4	Na+/K+ transporting ATPase interacting 4	NM_021426	-1.72516
Dlc1	deleted in liver cancer 1	NM_015802	-1.71766
Alox12	arachidonate 12-lipoxygenase	NM_007440	-1.71714
Syngr1	synaptogyrin 1	NM_207708	-1.71617
Ptprm	protein tyrosine phosphatase, receptor type, M	NM_008984	-1.71509
Cd109	CD109 antigen	NM_153098	-1.70606
Cpt1a	carnitine palmitoyltransferase 1a, liver	NM_013495	-1.70545
Igfbp3	insulin-like growth factor binding protein 3	NM_008343	-1.70523
Edil3	EGF-like repeats and discoidin I-like domains 3	NM_001037987	-1.7045

Prex1	phosphatidylinositol-3,4,5-trisphosphate-dependent Rac exchange factor 1	NM_177782	-1.70439
Aebp1	AE binding protein 1	NM_009636	-1.70392
Foxo1	forkhead box O1	NM_019739	-1.70091
Syde1	synapse defective 1, Rho GTPase, homolog 1 ( <i>C. elegans</i> )	NM_027875	-1.69704
Ica1	islet cell autoantigen 1	NM_010492	-1.69649
Faah	fatty acid amide hydrolase	NM_010173	-1.69601
Gsta3	glutathione S-transferase, alpha 3	NM_001077353	-1.69572
Renbp	renin binding protein	NM_023132	-1.69342
Gpr143	G protein-coupled receptor 143	NM_010951	-1.6893
Rab27b	RAB27b, member RAS oncogene family	NM_001082553	-1.68653
Cotl1	coactosin-like 1 ( <i>Dictyostelium</i> )	NM_028071	-1.68495
Gpr115	G protein-coupled receptor 115	NM_030067	-1.68479
Pla2g4f	phospholipase A2, group IVF	NM_001024145	-1.6837
Creg1	cellular repressor of E1A-stimulated genes 1	NM_011804	-1.68105
Atp6v0a1	ATPase, H <sup>+</sup> transporting, lysosomal V0 subunit A1	NM_016920	-1.68015
Fbn2	fibrillin 2	NM_010181	-1.67988
Cdkn1a	cyclin-dependent kinase inhibitor 1A (P21)	NM_007669	-1.67904
Abtb2	ankyrin repeat and BTB (POZ) domain containing 2	NM_178890	-1.67736
Vat1	vesicle amine transport protein 1 homolog ( <i>T californica</i> )	NM_012037	-1.67695
Agtr1a	angiotensin II receptor, type 1a	NM_177322	-1.67621
Rarb	retinoic acid receptor, beta	NM_011243	-1.67254
Tmbim1	transmembrane BAX inhibitor motif containing 1	NM_027154	-1.66823
Myo5b	myosin VB	NM_201600	-1.6682
Sdc3	syndecan 3	NM_011520	-1.66804
Fam83a	family with sequence similarity 83, member A	NM_173862	-1.66613
Aldh1a7	aldehyde dehydrogenase family 1, subfamily A7	NM_011921	-1.65783
Npl	N-acetylneuraminate pyruvate lyase	NM_028749	-1.65692
Nkd1	naked cuticle 1 homolog ( <i>Drosophila</i> )	NM_027280	-1.65403
Mall	mal, T-cell differentiation protein-like	NM_145532	-1.65312
Rehn	reelin	NM_011261	-1.65289
Rhob	ras homolog gene family, member B	NM_007483	-1.6515
Gm2a	GM2 ganglioside activator protein	NM_010299	-1.64723
Plbd1	phospholipase B domain containing 1	NM_025806	-1.64712
Gm6181	predicted pseudogene 6181	XM_885168	-1.64469
Prkg2	protein kinase, cGMP-dependent, type II	NM_008926	-1.64465
Fez1	fasciculation and elongation protein zeta 1 (zygin I)	NM_183171	-1.64201
Ppfibp2	PTPRF interacting protein, binding protein 2	NM_008905	-1.64072

	(liprin beta 2)		
Masp1	mannan-binding lectin serine peptidase 1	NM_008555	-1.64019
Palld	palladin, cytoskeletal associated protein	NM_001081390	-1.63705
Liph	lipase, member H	NM_001083894	-1.6357
B4galt5	UDP-Gal:betaGlcNAc beta 1,4-galactosyltransferase, polypeptide 5	NM_019835	-1.63195
Id2	inhibitor of DNA binding 2	NM_010496	-1.63144
Mxra7	matrix-remodelling associated 7	NM_026280	-1.63076
Ap1s2	adaptor-related protein complex 1, sigma 2 subunit	NM_026887	-1.62928
Slc27a6	solute carrier family 27 (fatty acid transporter), member 6	NM_001081072	-1.62671
Gfra1	glial cell line derived neurotrophic factor family receptor alpha 1	NM_010279	-1.62607
Serpinb7	serine (or cysteine) peptidase inhibitor, clade B, member 7	NM_027548	-1.62578
4930485B16Rik	RIKEN cDNA 4930485B16 gene	ENSMUST0000006770 5	-1.62514
Npr2	natriuretic peptide receptor 2	NM_173788	-1.62372
Fads3	fatty acid desaturase 3	NM_021890	-1.62337
Ankrd22	ankyrin repeat domain 22	NM_024204	-1.62334
Bend6	BEN domain containing 6	NM_177235	-1.6224
Cpeb4	cytoplasmic polyadenylation element binding protein 4	NM_026252	-1.62213
Nipal2	NIPA-like domain containing 2	NM_145469	-1.62162
Cpne4	copine IV	NM_028719	-1.62158
Serpina3b	serine (or cysteine) peptidase inhibitor, clade A, member 3	NM_173024	-1.62112
1700055N04Rik	RIKEN cDNA 1700055N04 gene	AK081788	-1.62076
Gm10786	predicted gene 10786	ENSMUST0000009955 0	-1.61909
Ppl	periplakin	NM_008909	-1.61745
Lta4h	leukotriene A4 hydrolase	NM_008517	-1.61696
Lpcat2	lysophosphatidylcholine acyltransferase 2	NM_173014	-1.61627
Tmem108	transmembrane protein 108	NM_178638	-1.61446
Ttc22	tetratricopeptide repeat domain 22	NM_177667	-1.6136
Fmod	fibromodulin	NM_021355	-1.6126
Sat1	spermidine/spermine N1-acetyl transferase 1	NM_009121	-1.61253
Lipk	lipase, family member K	NM_172837	-1.61147
Shc3	src homology 2 domain-containing transforming protein C3	NM_009167	-1.60699
Ahr	aryl-hydrocarbon receptor	NM_013464	-1.60638
Gucy1a3	guanylate cyclase 1, soluble, alpha 3	NM_021896	-1.60579
Dsg3	desmoglein 3	NM_030596	-1.6046
Tdrkh	tudor and KH domain containing protein	NM_028307	-1.60207

Tacstd2	tumor-associated calcium signal transducer 2	NM_020047	-1.60099
Tec	tec protein tyrosine kinase	NM_001113460	-1.60042
Scly	selenocysteine lyase	NM_016717	-1.59996
Mc1r	melanocortin 1 receptor	NM_008559	-1.59962
Gpr87	G protein-coupled receptor 87	NM_032399	-1.59921
Klhl30	kelch-like 30 (Drosophila)	NM_027551	-1.59911
Dact1	dapper homolog 1, antagonist of beta-catenin (xenopus)	NM_021532	-1.59768
Grhl1	grainyhead-like 1 (Drosophila)	NM_001161406	-1.59755
Thrb	thyroid hormone receptor beta	NM_009380	-1.59645
Ehd4	EH-domain containing 4	NM_133838	-1.5963
Klf3	Kruppel-like factor 3 (basic)	NM_008453	-1.5948
Col8a1	collagen, type VIII, alpha 1	NM_007739	-1.5946
Hoxc13	homeobox C13	NM_010464	-1.59267
Aqp3	aquaporin 3	NM_016689	-1.59194
Irak4	interleukin-1 receptor-associated kinase 4	NM_029926	-1.59068
Gm106	predicted gene 106	NM_001033288	-1.58707
Cbs	cystathionine beta-synthase	NM_144855	-1.58694
Dock10	dedicator of cytokinesis 10	NM_175291	-1.58613
I730030J21Rik	RIKEN cDNA I730030J21 gene	ENSMUST0000008925 2	-1.58459
Rnf128	ring finger protein 128	NM_023270	-1.58383
Mlph	melanophilin	NM_053015	-1.58285
Tacc1	transforming, acidic coiled-coil containing protein 1	NM_177089	-1.58058
Sult2b1	sulfotransferase family, cytosolic, 2B, member 1	NM_017465	-1.57843
Mrps21	mitochondrial ribosomal protein S21	NM_078479	-1.57721
Il1f5	interleukin 1 family, member 5 (delta)	NM_001146087	-1.57106
Pip5k1b	phosphatidylinositol-4-phosphate 5-kinase, type 1 beta	NM_008846	-1.5667
Cd63	CD63 antigen	NM_001042580	-1.56621
Egfl6	EGF-like-domain, multiple 6	NM_019397	-1.56356
Dnase1l3	deoxyribonuclease 1-like 3	NM_007870	-1.56243
Itm2a	integral membrane protein 2A	NM_008409	-1.56183
Susd2	sushi domain containing 2	NM_027890	-1.55929
D7Erttd443e	DNA segment, Chr 7, ERATO Doi 443, expressed	GQ499374	-1.55884
Maob	monoamine oxidase B	NM_172778	-1.5574
Cldn1	claudin 1	NM_016674	-1.55157
Nid1	nidogen 1	NM_010917	-1.5506
5430435G22Rik	RIKEN cDNA 5430435G22 gene	NM_145509	-1.55016
Nceh1	arylacetamide deacetylase-like 1	NM_178772	-1.5486
Eef2k	eukaryotic elongation factor-2 kinase	NM_007908	-1.54467
Ostf1	osteoclast stimulating factor 1	NM_017375	-1.54424

Serpinb3d	serine (or cysteine) peptidase inhibitor, clade B (ovalbumin) member 3	NM_201376	-1.54375
Trim71	tripartite motif-containing 71	NM_001042503	-1.54353
Lgals12	lectin, galactose binding, soluble 12	NM_019516	-1.5435
D030046N08Rik	RIKEN cDNA D030046N08 gene	AK141732	-1.54326
Cds1	CDP-diacylglycerol synthase 1	NM_173370	-1.54218
Lactb2	lactamase, beta 2	NM_145381	-1.5418
Runx3	runt related transcription factor 3	NM_019732	-1.54153
Abhd14b	abhydrolase domain containing 14b	NM_029631	-1.54123
Tinagl1	tubulointerstitial nephritis antigen-like 1	NM_023476	-1.53826
Aldh3b2	aldehyde dehydrogenase 3 family, member B2	NM_001177438	-1.53793
Sgpp1	sphingosine-1-phosphate phosphatase 1	NM_030750	-1.53666
Ndrg2	N-myc downstream regulated gene 2	NM_013864	-1.5341
Fam178b	family with sequence similarity 178, member B	NM_201365	-1.53347
9530008L14Rik	RIKEN cDNA 9530008L14 gene	NM_175417	-1.53333
Depdc6	DEP domain containing 6	NM_001037937	-1.53249
Elavl4	ELAV (embryonic lethal, abnormal vision, <i>Drosophila</i> )-like 4	NM_010488	-1.53164
Kcnk6	potassium inwardly-rectifying channel, subfamily K, member 6	NM_001033525	-1.53139
Trpc1	transient receptor potential cation channel, subfamily C, member 1	NM_011643	-1.53134
Pdzk1ip1	PDZK1 interacting protein 1	NM_001164557	-1.52907
Tubb3	tubulin, beta 3	NM_023279	-1.5283
Paqr5	progestin and adipoQ receptor family member V	NM_028748	-1.52822
Vegfc	vascular endothelial growth factor C	NM_009506	-1.52594
Myc	myelocytomatosis oncogene	NM_010849	-1.52588
Trim2	tripartite motif-containing 2	NM_030706	-1.52511
Trpm1	transient receptor potential cation channel, subfamily M, member 1	NM_001039104	-1.52394
Gstm6	glutathione S-transferase, mu 6	NM_008184	-1.52352
Gsdmc	gasdermin C	NM_031378	-1.52268
Rapgef1	Rap guanine nucleotide exchange factor (GEF)-like 1	NM_001080925	-1.52242
Tmem184a	transmembrane protein 184a	NM_001161548	-1.52236
Car6	carbonic anhydrase 6	NM_009802	-1.52167
Krt15	keratin 15	NM_008469	-1.51893
Dsc2	desmocollin 2	NM_013505	-1.51662
Tcn2	transcobalamin 2	NM_015749	-1.51643
Gstp2	glutathione S-transferase, pi 2	NM_181796	-1.51642
Lce6a	late cornified envelope 6A	NM_001166172	-1.51564
Vcan	versican	NM_001081249	-1.5153

Ahnak2	AHNAK nucleoprotein 2	BC138468	-1.51427
Retsat	retinol saturase all trans retinol 13,14 reductase	NM_026159	-1.51347
Rapgef4	Rap guanine nucleotide exchange factor (GEF) 4	NM_019688	-1.51327
Gltp	glycolipid transfer protein	NM_019821	-1.51324
Mcam	melanoma cell adhesion molecule	NM_023061	-1.51124
Sdr42e1	short chain dehydrogenase/reductase family 42E, member 1	NM_028725	-1.51123
Mmp16	matrix metallopeptidase 16	NM_019724	-1.51108
Sec11c	SEC11 homolog C ( <i>S. cerevisiae</i> )	NM_025468	-1.51074
Ltbr	lymphotoxin B receptor	NM_010736	-1.50968
Sptlc3	serine palmitoyltransferase, long chain base subunit 3	NM_175467	-1.50781
Thbd	thrombomodulin	NM_009378	-1.50665
Il17rc	interleukin 17 receptor C	NM_134159	-1.50461
Prrg4	proline rich Gla (G-carboxyglutamic acid) 4 (transmembrane)	NM_178695	-1.50406
2210411K11Rik	RIKEN cDNA 2210411K11 gene	NM_029384	-1.50405
Il1rap	interleukin 1 receptor accessory protein	NM_008364	-1.50257
Maoa	monoamine oxidase A	NM_173740	-1.50129
Notch3	Notch gene homolog 3 ( <i>Drosophila</i> )	NM_008716	-1.50126
Lmo4	LIM domain only 4	NM_010723	-1.5007

**Supplementary Table S2.** Representative lists of differentially regulated genes in the epidermis of  $\Delta N$  embryos when compared to controls at E14.5 (**a**, downregulated and **b**, upregulated in  $\Delta N$  embryos vs. controls). Only mRNAs differentially up- or down-regulated  $\geq 1.5x$  are listed.

### Differentially expressed genes in $\Delta N$ embryos at E14.5

#### a) Downregulated in $\Delta N$ embryos:

Genes symbol	Description	Ref_Seq	Fold change
Frem1	Fras1 related extracellular matrix protein 1	NM_177863	5.3297
Tnc	tenascin C	NM_011607	4.18183
Cd74	CD74 Antigen	NM_001042605	3.83445
Prnd	prion protein dublet	NM_023043	3.69287
Socs2	suppressor of cytokine signaling 2	NM_007706	3.64399
Dkk4	dickkopf homolog 4 (Xenopus laevis)	NM_145592	3.59292
Pla2g7	phospholipase A2, group VII (platelet-activating factor acetylhydrolase, plasma)	NM_013737	3.51707
Slc14a1	solute carrier family 14 (urea transporter), member 1	NM_001171010	3.42343
Ly6g6c	lymphocyte antigen 6 complex, locus G6C	NM_023463	3.03654
Foxi3	forkhead box I3	NM_001101464	2.90417
Serpinb3a	serine (or cysteine) peptidase inhibitor, clade B (ovalbumin) member 3	NM_009126	2.85518
Susd2	sushi domain containing 2	NM_027890	2.82966
Ptch1	patched homolog 1	NM_008957	2.82694
BC100530	cDNA sequence BC100530	NM_001082546	2.80312
Wif1	Wnt inhibitory factor 1	NM_011915	2.77261
Clca2	chloride channel calcium activated 2	NM_030601	2.69697
Nrp2	neuropilin 2	NM_001077403	2.64097
Necab1	N-terminal EF-hand calcium binding protein 1	NM_178617	2.63714
Lypd5	Ly6/Plaur domain containing 5	NM_029806	2.54125
Gli1	GLI-Kruppel family member GLI1	NM_010296	2.49257
Trps1	trichorhinophalangeal syndrome I (human)	NM_032000	2.47674
Dusp6	dual specificity phosphatase 6	NM_026268	2.46991
Il2rg	interleukin 2 receptor, gamma chain	NM_013563	2.4657
Tspan18	tetraspanin 18	NM_183180	2.4343
Serpinb2	serine (or cysteine) peptidase inhibitor, clade B, membebr 2	NM_001174170	2.39753
Tnf	tumor necrosis factor	NM_013693	2.38059
Acer1	alkaline ceramidase 1	NM_175731	2.37223

Adamts3	a disintegrin-like and metallopeptidase with thrombospondin motifs 3	NM_177872	2.21406
C1s	complement component 1, s subcomponent	NM_144938	2.21217
Rragd	Ras-related GTP binding D	NM_027491	2.20995
Ltb	lymphotoxin B	NM_008518	2.20462
Tprg	transformation related protein 63 regulated	NM_175165	2.17802
Sprr1b	small proline-rich protein 1B	NM_009265	2.16581
Stfa1	stefin A1	NM_001082543	2.16379
2610528A11Rik	RIKEN cDNA 2610528A11 gene	BC049685	2.13002
Sdr9c7	4short chain dehydrogenase/reductase family 9C, member 7	NM_027301	2.12331
Ptch2	patched homolog 2	NM_008958	2.11929
Ncam1	neural cell adhesion molecule 1	NM_001081445	2.11752
Sostdc1	sclerostin domain containing 1	NM_025312	2.10836
Krt77	keratin 77	NM_001003667	2.0926
Prss35	protease, serine, 35	NM_178738	2.05754
Srgap1	SLIT-ROBO Rho GTPase activating protein 1	NM_001081037	2.04739
Fndc1	fibronectin type III domain containing 1	NM_001081416	2.01216
D19Ert652e	DNA segment, Chr 19, ERATO Doi 652, expressed	BC107403	1.98524
4833423E24Rik	RIKEN cDNA 4833423E24 gene	NM_001081664	1.98148
Aox4	aldehyde oxidase 4	NM_023631	1.97771
Tnfaip3	tumor necrosis factor, alpha-induced protein 3	NM_009397	1.94167
Galnt6	UDP-N-acetyl-alpha-D-galactosamine: polypeptide N-acetylgalactosaminyltransferase 6	NM_001161767	1.91422
2210023G05Rik	RIKEN cDNA 2210023G05 gene	NM_197999	1.90753
Fgd5	FYVE, RhoGEF and PH domain containing 5	NM_172731	1.90493
Eif4e3	eukaryotic translation initiation factor 4E member 3	NM_025829	1.89894
Cyfip2	cytoplasmic FMR1 interacting protein 2	NM_133769	1.89842
Ifitm1	interferon induced transmembrane protein 1	NM_026820	1.89673
Cntnap1	contactin associated protein-like 1	NM_016782	1.89603
Egln3	EGL nine homolog 3 (C. elegans)	NM_028133	1.88526
Bcar3	breast cancer anti-estrogen resistance 3	NM_013867	1.86971
Shh	sonic hedgehog	NM_009170	1.86585
Madcam1	mucosal vascular addressin cell adhesion molecule 1	NM_013591	1.86208
Mical2	microtubule associated monooxygenase, calponin and LIM domain containing 2	NM_177282	1.84081
Vldlr	very low density lipoprotein receptor	NM_013703	1.83891

Robo2	roundabout homolog 2 ( <i>Drosophila</i> )	NM_175549	1.83432
Cyp17a1	cytochrome P450, family 17, subfamily a, polypeptide 1	NM_007809	1.83325
Lor	loricrin	NM_008508	1.83189
Stfa3	stefin A3	NM_025288	1.82883
Serpinb3b	serine (or cysteine) peptidase inhibitor, clade B (ovalbumin) member 3	NM_198680	1.82336
Clca1	chloride channel calcium activated 1	NM_009899	1.82303
Cnfn	cornifelin	NM_028219	1.81784
Serpinb3c	serine (or cysteine) peptidase inhibitor, clade B (ovalbumin) member 3	NM_201363	1.80208
Sdr16c5	short chain dehydrogenase/reductase family 16C, member 5	NM_181989	1.79991
Etv4	ets variant gene 4 (E1A enhancer binding protein, E1AF)	NM_008815	1.79859
Chl1	cell adhesion molecule with homology to L1CAM	NM_007697	1.78983
Mmp9	matrix metallopeptidase 9	NM_013599	1.78771
Moxd1	monooxygenase, DBH-like 1	NM_021509	1.78575
Etv5	ets variant gene 5	NM_023794	1.77897
1600029D21Rik	RIKEN cDNA 1600029D21 gene	NM_029639	1.7675
Alox12b	arachidonate 12-lipoxygenase, 12R type	NM_009659	1.7653
Tmem45a	transmembrane protein 45a	NM_019631	1.76028
Bcl3	B-cell leukemia/lymphoma 3	NM_033601	1.75433
Rgs5	regulator of G-protein signaling 5	NM_009063	1.72895
Astl	astacin-like metalloendopeptidase (M12 family)	NM_172539	1.72024
Lgals3	lectin, galactose binding, soluble 3	NM_001145953	1.71812
Ndufa4l2	NADH dehydrogenase (ubiquinone) 1 alpha subcomplex, 4-like 2	NM_001098789	1.71246
Prokr2	prokineticin receptor 2	NM_144944	1.7097
Csf1	colony stimulating factor 1 (macrophage)	NM_007778	1.70757
Mtmar10	myotubularin related protein 10	NM_172742	1.68499
Relb	avian reticuloendotheliosis viral (v-rel) oncogene related homolog B	NM_009046	1.68204
Ifitm3	interferon induced transmembrane protein 3	NM_025378	1.67277
Npl	N-acetylneuraminate pyruvate lyase	NM_028749	1.67257
Ephx3	epoxide hydrolase 3	NM_001033163	1.67166
Tmem176a	transmembrane protein 176A	NM_025326	1.66412
Nrp1	neuropilin 1	NM_008737	1.6554
B2m	beta-2 microglobulin	NM_009735	1.65432
Aadacl2	arylacetamide deacetylase-like 2	NM_001128091	1.65394

Serpinb5	serine (or cysteine) peptidase inhibitor, clade B, member 5	NM_009257	1.65227
Serpinb6b	serine (or cysteine) peptidase inhibitor, clade B, member 6	NM_011454	1.6513
Me1	malic enzyme 1, NADP(+)-dependent, cytosolic	NM_008615	1.6483
Adamts15	a disintegrin-like and metallopeptidase with thrombospondin motifs 15	NM_001024139	1.64688
Sbsn	suprabasin	NM_172205	1.64486
Alox12e	arachidonate lipoxygenase, epidermal	NM_145684	1.64479
Tgfb1	transforming growth factor, beta 1	NM_011577	1.64403
Mest	mesoderm specific transcript	NM_008590	1.64183
Setbp1	SET binding protein 1	NM_053099	1.62694
Steap4	STEAP family member 4	NM_054098	1.62451
Serpinb3d	serine (or cysteine) peptidase inhibitor, clade B (ovalbumin) member 3	NM_201376	1.62108
Tmem176b	transmembrane protein 176B	NM_023056	1.6186
Ikbke	inhibitor of kappaB kinase epsilon	NM_019777	1.61781
Elovl7	ELOVL family member 7, elongation of long chain fatty acids	NM_029001	1.61718
Ankrd35	ankyrin repeat domain 35	NM_001081139	1.6135
Cxcl11	chemokine (C-X-C motif) ligand 11	NM_019494	1.60827
Ptges	prostaglandin E synthase	NM_022415	1.60778
Osmr	oncostatin M receptor	NM_011019	1.6042
Calml3	calmodulin-like 3	NM_027416	1.6038
Pthlh	parathyroid hormone-like peptide	NM_008970	1.60116
Lipm	lipase, family member M	NM_023903	1.60038
Orm1	orosomucoid 1	NM_008768	1.59549
Kcnip3	Kv channel interacting protein 3, calsenilin	NM_019789	1.58749
Phyhip	phytanoyl-CoA hydroxylase interacting protein	NM_145981	1.57769
Trim25	tripartite motif-containing 25	NM_009546	1.57537
Serpinb12	serine (or cysteine) peptidase inhibitor, clade B (ovalbumin) member 12	NM_027971	1.57423
Adra2b	adrenergic receptor, alpha 2b	NM_009633	1.57349
Pla2g2f	phospholipase A2, group IIF	NM_012045	1.56977
Mapk4	mitogen-activated protein kinase 4	NM_172632	1.56745
Them5	thioesterase superfamily member 5	NM_025416	1.56526
Glul	glutamate-ammonia ligase (glutamine synthetase)	NM_008131	1.56162
Cspg4	chondroitin sulfate proteoglycan 4	NM_139001	1.55824
Rasgrp1	RAS guanyl releasing protein 1	NM_011246	1.55786
F3	coagulation factor III	NM_010171	1.55233

Ttc39b	tetratricopeptide repeat domain 39B	NM_027238	1.54678
Stard5	StAR-related lipid transfer (START) domain containing 5	NM_023377	1.54597
Gsdmc	gasdermin C	NM_031378	1.54584
Trex2	three prime repair exonuclease 2	NM_011907	1.54408
Clca5	chloride channel calcium activated 5	NM_178697	1.54023
Arhgef3	Rho guanine nucleotide exchange factor (GEF) 3	NM_027871	1.53812
Rdh12	retinol dehydrogenase 12	NM_030017	1.53806
Dapl1	death associated protein-like 1	NM_029723	1.53781
Serpinb7	serine (or cysteine) peptidase inhibitor, clade B, member 7	NM_027548	1.53095
Parp12	poly (ADP-ribose) polymerase family, member 12	NM_172893	1.52898
Figf	c-fos induced growth factor	NM_010216	1.52603
Bnip3	BCL2/adenovirus E1B interacting protein 3	NM_009760	1.5244
Pdzk1ip1	PDZK1 interacting protein 1	NM_001164557	1.52419
Myb	myeloblastosis oncogene	NM_010848	1.52289
Lhx2	LIM homeobox protein 2	NM_010710	1.52144
Zdhhc2	zinc finger, DHHC domain containing 2	NM_178395	1.51928
Stra6	stimulated by retinoic acid gene 6	NM_009291	1.51604
Gsta1	glutathione S-transferase, alpha 1 (Ya)	NM_008181	1.5139
Acta2	actin, alpha 2, smooth muscle, aorta	NM_007392	1.51301
Car13	carbonic anhydrase 13	NM_024495	1.51048
Krt16	keratin 16	NM_008470	1.50953
Acsl1	acyl-CoA synthetase long-chain family member 1	NM_007981	1.50813
Gpm6b	glycoprotein m6b	NM_001177956	1.50714
Cxcl9	chemokine (C-X-C motif) ligand 9	NM_008599	1.5062
Tnip1	TNFAIP3 interacting protein 1	NM_021327	1.50449
Itpkb	inositol 1,4,5-trisphosphate 3-kinase B	NM_001081175	1.50267
Ptgs1	prostaglandin-endoperoxide synthase 1	NM_008969	1.50105
Sox9	SRY-box containing gene 9	NM_011448	1.50071
Acsl4	acyl-CoA synthetase long-chain family member 4	NM_207625	1.50053
Cald1	caldesmon 1	NM_145575	1.50041

**b) Upregulated in  $\Delta N$  embryos:**

Genes symbol	gene_assignment	Ref seq	Fold change
Gm10304	predicted gene 10304	ENSMUST00000 94945	-3.26077

Mybpc1	myosin binding protein C, slow-type	NM_175418	-3.25459
Gm9911	predicted gene 9911	AK035883	-2.6811
Pcsk2	proprotein convertase subtilisin/kexin type 2	NM_008792	-2.5787
Igfbp3	insulin-like growth factor binding protein 3	NM_008343	-2.25564
Pisd-ps2	phosphatidylserine decarboxylase, pseudogene 2	NR_003519	-2.21286
St6galnac2	ST6 (Alpha-N-Acetyl-Neuraminyl-2,3-Beta-Galactosyl-1,3)-N-Acetylgalactosaminide Alpha-2,6-Sialyltransferase 2	NM_009180	-2.20545
Elmo1	engulfment and cell motility 1, ced-12 homolog (C. elegans)	NM_080288	-2.13654
Unc5d	unc-5 homolog D (C. elegans)	NM_153135	-2.13157
Lrrn1	leucine rich repeat protein 1, neuronal	NM_008516	-2.10864
Ano4	anoctamin 4	NM_178773	-2.05626
Jun	Jun oncogene	NM_010591	-2.03491
Kcnh7	potassium voltage-gated channel, subfamily H (eag-related) member 7	NM_133207	-1.98255
Cd68	CD68 antigen	NM_009853	-1.89433
Mir19b-1	microRNA 19b-1	NR_029815	-1.82456
Gria2	glutamate receptor, ionotropic, AMPA2 (alpha 2)	NM_013540	-1.78212
Lix1	limb expression 1 homolog (chicken)	NM_025681	-1.77782
Slc24a3	solute carrier family 24 (sodium/potassium/calcium exchanger) member 3	NM_053195	-1.76643
Spo11	sporulation protein, meiosis-specific, SPO11 homolog	NM_012046	-1.74945
Cygb	cytoglobin	NM_030206	-1.74346
Igf1	insulin-like growth factor 1	NM_010512	-1.74324
Npbwr1	neuropeptides B/W receptor 1	NM_010342	-1.73667
Scube1	signal peptide, CUB domain, EGF-like 1	NM_022723	-1.72514
Slc4a4	solute carrier family 4 (anion exchanger), member 4	NM_018760	-1.72296
1700001P01Rik	RIKEN cDNA 1700001P01 gene	NM_028156	-1.68043
Plcd2	phosphatidylinositol-specific phospholipase C, X domain containing 2	NM_001134480	-1.67512
Bmp2	bone morphogenetic protein 2	NM_007553	-1.66547
Lrch2	leucine-rich repeats and calponin homology (CH) domain containing 2	NM_001081173	-1.66022
B230325K18Rik	RIKEN cDNA B230325K18 gene	ENSMUST00000079045	-1.65577
AY512949	cDNA sequence AY512949	AY512949	-1.6508
Thsd7b	thrombospondin, type I, domain containing 7B	NM_172485	-1.64462
Lce6a	late cornified envelope 6A	NM_001166172	-1.63186
Pcdh10	protocadherin 10	NM_001098171	-1.63084

Sprr2a1	small proline-rich protein 2A1	AY158986	-1.61029
Fam38b	family with sequence similarity 38, member B	NM_001039485	-1.6021
Mirlet7c-1	microRNA let7c-1	NR_029728	-1.59206
Cd96	CD96 antigen	NM_032465	-1.58805
Snora75	small nucleolar RNA, H/ACA box 75	NR_028478	-1.56597
Pcdh17	protocadherin 17	NM_001013753	-1.56052
Ripply3	ripply3 homolog (zebrafish)	NM_133229	-1.55827
Cdh6	cadherin 6	NM_007666	-1.55706
Dusp1	dual specificity phosphatase 1	NM_013642	-1.55033
Tagln3	transgelin 3	NM_019754	-1.54993
Col19a1	collagen, type XIX, alpha 1	NM_007733	-1.54267
Nkain2	Na+/K+ transporting ATPase interacting 2	NM_001013411	-1.52611
Gm12703	predicted gene 12703	ENSMUST00000 064804	-1.526
Baalc	brain and acute leukemia, cytoplasmic	NM_080640	-1.51608
Ica1	islet cell autoantigen 1	NM_010492	-1.51287
Igfbp2	insulin-like growth factor binding protein 2	NM_008342	-1.51232
Snhg1	small nucleolar RNA host gene (non-protein coding) 1	AK051045	-1.51117
Gpx6	glutathione peroxidase 6	NM_145451	-1.51012
Taf1d	TATA box binding protein (Tbp)-associated factor, RNA polymerase I D	AK161656	-1.50123
Adam1a	a disintegrin and metallopeptidase domain 1a	NM_172126	-1.50059

**Supplementary Table S3. Upper table:** Number of NF-κB binding sites and cross-species conservation of all primary hair follicle placode-specific NF-κB target genes that have been analysed by qRT-PCR and ChIP (*Lhx2*, *Sox9*, *Mmp9*, *Trps1*) using an anti-p65 antibody. The right column indicates whether a particular gene was also bound by NF-κB subunits in Hodgkin's lymphoma cell lines (E. Kärgel and C. Scheidereit, unpublished). Previously unknown NF-κB targets are marked in green (see also <http://www.bu.edu/nf-kb/gene-resources/target-genes/>). **Lower table:** Cross-species conservation and number of LHX2 binding sites in NF-κB targets *Nrp2* and *Prokr2*.

Gene symbol	Number of potential NF-κB binding sites - JASPER (> 90%)	Cross species conservation - ECR browser Dcode	ChIP peak of NF-κB subunits in Hodgkin lymphoma
Adamts3	3	Binding sites are conserved in Muroidea	-
Adamts15	6	Binding sites are conserved in Muroidea	-
Ascl4	0	-	-
Bcl3	5	Binding sites are conserved up to Metatheria	Yes
Bmp2	2	Binding sites are conserved in Mammals	-
<b>Cd74</b>	4	Binding sites are conserved up to Metatheria	Yes
Cxcl9	8	Binding sites are conserved in Mammals	-
Cxcl11	7	Binding sites are conserved in Mammals	-
Dkk4	2	-	-
Dusp6	2	Binding sites are conserved in Vertebrata	Yes
<b>Etv4</b>	3	Binding sites are conserved up to Metatheria	Yes
<b>Etv5</b>	1	-	-
Fndc1	17	Binding sites are conserved in Muroidea	-
Foxi3	0	-	-
Frem1	10	Binding sites are conserved in Mammals	-
<b>Galnt6</b>	7	Binding sites are conserved in Mammals	Yes
Gli1	2	Binding sites are conserved in Mammals	Yes
Krt17	5	Binding sites are conserved in Muroidea	-
<b>Lhx2</b>	7	Binding sites are conserved in Mammals	Yes
Ltb	1	Binding site is conserved in Mammals	Yes
Madcam1	3	Binding sites are conserved in Muroidea	Yes
<b>Mical2</b>	18	Binding sites are conserved in Muroidea	Yes
Mmp9	3	Binding sites are conserved in Mammals	Yes
Ncam1	26	Binding sites are conserved in Mammals	Yes
<b>Nrp2</b>	16	Binding sites are conserved in Mammals	Yes
Prokr2	5	Binding sites are conserved in Muroidea	-
Prss35	3	-	-
<b>Ptch1</b>	2	Binding sites are conserved in Mammals	Yes
Ptch2	5	-	-
Pthlh	2	Binding sites are conserved in Mammals	Yes

<b>Robo2</b>	32	Binding sites are conserved in Muroidea	Yes
<b>Scube1</b>	20	Binding sites are conserved in Muroidea	Yes
Shh	4	Binding sites are conserved in Mammals	Yes
Socs2	3	Binding sites are conserved in Mammals	-
Sox9	2	Binding sites are conserved in Mammals	Yes
Sox21	2	Binding sites are conserved in Vertebrata	-
<b>Srgap1</b>	3	Binding sites are conserved in Mammals	Yes
<b>Tgfb1</b>	2	Binding sites are conserved in Muroidea	Yes
Tnc	3	Binding sites are conserved in Mammals	Yes
Tnf	3	Binding sites are conserved in Mammals	Yes
Tnfaip3	9	Binding sites are conserved up to Aves	Yes
<b>Trps1</b>	7	Binding sites are conserved up to Aves	Yes
Tsku	3	-	-
<b>Tspan18</b>	18	Binding sites are conserved in Mammals	Yes
Wif1	3	Binding sites are conserved in Muroidea	-
Wnt2b	1	Binding site is conserved in Mammals	-
<b>Total</b>	<b>44 of 46 ~ 96%</b>		<b>26 of 46 ~ 57%</b>

<b>Gene symbol</b>	<b>Number of potential LHX2 binding sites - JASPER (&gt; 90%)</b>	<b>Cross species conservation - ECR browser Dcode</b>
Nrp2	6	Binding sites are conserved in Muroidea
Prokr2	1	Binding sites are not conserved

**Supplementary Table S4.** List of genes specifically upregulated in the interfollicular epidermis (IFE), but down-regulated by NF- $\kappa$ B in hair follicle placodes at E14.5.

**Genes specifically upregulated in the interfollicular epidermis (IFE) and down-regulated by NF- $\kappa$ B in hair follicle placodes**

Genes symbol	Description	Ref seq	Fold change (WT vs. $\Delta N$ )	Fold change (HF vs IFE)
Pcsk2	proprotein convertase subtilisin/kexin type 2	NM_008792	-2.5787	-2.04744
Igfbp3	insulin-like growth factor binding protein 3	NM_008343	-2.25564	-1.70523
Igf1	insulin-like growth factor 1	NM_010512	-1.74324	-2.19222
Npbwr1	neuropeptides B/W receptor 1	NM_010342	-1.73667	-1.9776
Lce6a	late cornified envelope 6A	NM_001166172	-1.63186	-1.51564
Ica1	islet cell autoantigen 1	NM_010492	-1.51287	-1.69649